JOURNAL OF MOLECULAR SPECTROSCOPY **179,** 41–60 (1996)
ARTICLE NO. 0182

The Third and Fourth Torsional States of Acetaldehyde

I. Kleiner,* J. T. Hougen,† J.-U. Grabow,† S. P. Belov,‡ M. Yu. Tretyakov,‡ and J. Cosléou¶

*Laboratoire de Physique Moléculaire et Applications, Université Pierre et Marie Curie, Unité Propre du CNRS (Laboratoire associé aux Universités P. et M. Curie et Paris XI), Tour 13, 4, Place Jussieu, Bte. 76, F-75252 Paris Cedex 05, France; †Molecular Physics Division, National Institute of Standards and Technology, Gaithersburg, Maryland 20899; ‡Microwave Spectroscopy Division, Applied Physics Institute, 46 Ulyanova Street, Nizhny Novgorod, Russia 603024; and ¶Laboratoire de Spectroscopie Hertzienne, Université des Sciences et Techniques de Lille, 59655 Villeneuve d'Ascq Cedex, France

Received February 5, 1996

A least-squares fit is presented of 1105 far-infrared and 2860 microwave transitions in acetaldehyde, which sample rotational levels in all torsional states below the lowest-frequency small-amplitude vibration ν_{10}. Four-fifths of these transitions, involving torsional states below the barrier ($v_t \leqslant 2$), were treated in an earlier publication; here the theoretical model is further tested by extending the data set to include the $v_t = 3$ and 4 states above the barrier. The new data set includes (i) 224 $v_t = 3 \leftarrow 2$ far-infrared transitions, (ii) Nizhny Novgorod RAD-2 *a*-type and *b*-type submillimeter transitions in $v_t = 2$, which make more precise $\Delta K = \pm 1$ intervals in this last torsional state below the barrier, (iii) RAD-3 *a*-type submillimeter transitions in $v_t = 3$ and 4, and (iv) microwave and submillimeter measurements or remeasurements from NIST and Lille of transitions with $v_t \leqslant 4$. The global fit, which uses an improved version of the computer program previously applied to the $v_t \leqslant 2$ data, gave a weighted overall standard deviation of 1.21 with 55 adjusted and 2 fixed parameters. Residuals from the fit were close to experimental uncertainties for the infrared wavenumber measurements and for microwave and submillimeter frequency measurements below the barrier, but some residuals reached several MHz or more for frequency measurements involving levels near ν_{10}. We have attempted to achieve a qualitative understanding of the numerical results by presenting a general overview of internal rotation energy levels above the barrier and a theoretical discussion of torsion–rotation interactions among these levels.

1. INTRODUCTION

In the previous paper (*5*) of this series (*1–5*), we presented a global fit, essentially to experimental accuracy, of transitions in acetaldehyde involving all three torsional states below the barrier, i.e., $v_t = 0$, 1, and 2. This combined *A* and *E* species fit of 2284 microwave and millimeter-wave lines and 824 far-infrared lines to 48 parameters gave a weighted standard deviation of 1.06.

In this paper we consider part of the first ($v_t = 3$) and second ($v_t = 4$) torsional states above the barrier, presenting (i) a theoretical discussion of the approximate energy level structure expected as the free-rotor limit is approached, (ii) a detailed spectroscopic analysis and global fit of the previous data set augmented by several hundred infrared and microwave transitions involving the $v_t = 3$ *A* and *E* torsional components together with a limited number of microwave lines in the $v_t = 4$ state, and (iii) a discussion of various torsion–rotation interactions contributing to quantum-mechanical and spectral complexity for energy levels above the barrier.

Since the model used for the present study does not allow for interaction of small-amplitude vibrations with nearby torsional states, we limit consideration in this paper to torsional *K*-stacks whose (hypothetical) $J = 0$ energy lies below the lowest small-amplitude mode, ν_{10}, at 509 cm^{-1}. A large number of assignments and a relatively good fit (with most $v_t = 3$ and 4 deviations less than a few MHz) are presented, which give us our first concrete understanding of the variety and magnitude of torsion–rotation interactions actually present above the barrier in acetaldehyde and which permit detailed planning of experiments designed to elucidate the perturbations associated with many of these interactions.

2. COMPARISON OF TORSION–ROTATION LEVELS BELOW AND ABOVE THE BARRIER

An overview of the qualitative energy level changes that occur in a methyl-rotor internal rotation problem as the amount of energy in the torsional degree of freedom increases can be obtained by examining Fig. 1, which displays as a function of $K \leqslant 20$ a number of energy levels obtained from the approximate torsion–*K*-rotation Hamiltonian

$$\begin{aligned} H_{tKr} &= F(P_\gamma + \rho J_z)^2 + \tfrac{1}{2}V_3(1 - \cos 3\gamma) \\ &\quad + [A - (B + C)/2]J_z^2 \\ &\equiv H_{tor}(F, V_3, \rho) + H_{K-rot}(A, B, C), \end{aligned} \tag{1}$$

where *A*, *B*, *C* are the usual asymmetric-rotor rotational constants, V_3 is the threefold barrier height, *F* is the rotational

0022-2852/96 $18.00

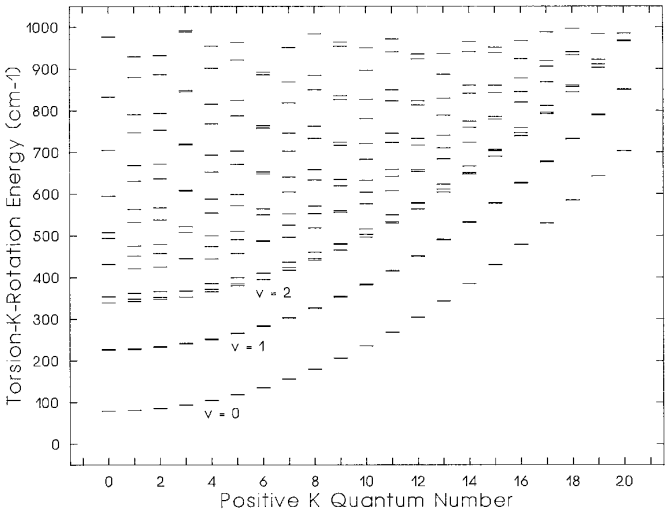

FIG. 1. Low-lying ''torsion–*K*-rotation'' energy levels for a system exhibiting internal rotation and overall *K* rotation (two degrees of freedom), calculated from the Hamiltonian H_{tKr} in Eq. [1] using $F = 7.656$ cm^{-1}, $V_3 = 408$ cm^{-1}, $\rho = 0.3291$, and $A - (B + C)/2 = 1.559$ cm^{-1}, as appropriate for acetaldehyde. Energy levels for the torsional quantum numbers $v_t = 0$, 1, and 2 lie on clearly visible parabolas when plotted against *K*, corresponding to approximate energy expressions of the form $E_{\text{torsion}} + [A - (B + C)/2]K^2$. For these $v_t \leqslant 2$ levels E_{torsion} is less than the torsional barrier height. Significant internal rotation splittings can only be seen in the $v_t = 2$ levels, for which E_{torsion} approaches the top of the barrier. Levels with torsional energies greater than the barrier height do not fall into such simple patterns, and they are not labeled in this figure.

constant associated with internal rotation, and ρ is a structural parameter involving moments of inertia of the top and frame in the molecule. (Note that for easier comparison with our computer output, we have chosen the plus sign convention between P_γ and ρJ_z, which is opposite to the sign choice in some other papers (*6*, *7*).) Values for molecular parameters appropriate for acetaldehyde were taken from Table I of Ref. (*5*) and used in Eq. [1] to generate Fig. 1, which thus displays the hypothetical $J = 0$ level for each *K* and torsional state.

Torsional splittings in the levels for $v_t = 0$ and 1 are mostly too small to be seen in Fig. 1, so these levels appear to have energies given simply by

$$E_{K-\text{rot}} = [A - (B + C)/2]K^2 \qquad [2]$$

plus an additive constant E_{tor} representing the vibrational energy of the torsional state v_t. For $v_t = 2$, the last level below the top of the barrier, torsional splittings of the levels into doublets and triplets can clearly be seen superimposed on the level pattern of Eq. [2]. Torsional contributions to the energies for $v_t = 0$, 1, and 2 are given (with the sign conventions in our computer program) by a Fourier cosine series of the form (*7*)

$$E_{\text{tor}} = \sum_n F a_n^{(v_t)} \cos[(2\pi n/3)(K\rho + \sigma)], \qquad [3]$$

where the $n = 0$ constant term represents the vibrational energy of the torsional state v_t, and the sum of all higher *n* terms represents the torsional splitting in this state as a function of *K* and σ. (The maximum value of *n* required in the series depends on the magnitude of the splitting and the desired accuracy.) Values of $\sigma = 0$ and ± 1 correspond to levels of *A* and *E* symmetry, respectively, in the G_6 molecular symmetry group appropriate for the internal rotation problem in acetaldehyde. The general properties of torsion–*K*-rotation levels described by the sum of Eqs. [2] and [3], i.e., levels below the barrier, will not be considered further in this paper.

Instead, we focus on levels above the barrier, i.e., on the levels lying above $v_t = 2$ in Fig. 1. These show much less regularity than the lower v_t levels, but they can be organized from a free-rotor point of view by reasoning as follows. In the free-rotor limit, effects of the barrier can be neglected, and torsion–K-rotation levels from Eq. [1] are given by an expression of the form

$$E(m,K) = F(m + \rho K)^2 + [A - (B + C)/2]K^2, \qquad [4]$$

where $m = 0, \pm 1, \pm 2, \ldots$ is the free-rotor quantum number. All of these free-rotor torsion–*K*-rotation energy levels, except for $m = K = 0$, are doubly degenerate since $E(m,K) = E(-m, -K)$.

As usual when passing from one limiting case to another, there is an intermediate region where energy levels are given neither by the sum of Eqs. [2] and [3] nor by Eq. [4]. For this region it is useful to determine the correlation between the torsional *vibrational* quantum number v_t, appropriate well below the barrier, and the internal rotation *free-rotor* quantum number *m*, appropriate well above the barrier. This correlation, which depends also on the symmetry species of the level, is given in Table 1. For the acetaldehyde levels in Fig. 1, it would be possible to change from vibrational to free-rotor quantum number labels above about $v_t = 3$ or 4. Some aspects of the approximate quantum number *m* in the $v_t \rightarrow m$ changeover region are discussed below, particularly the use of signed *m* and positive *K* values when torsion–*K*-rotation interaction is large enough to split torsional *E* states ($m \neq 0$ mod 3) and mix close-lying torsional A_1, A_2 pairs ($m = 0$ mod 3). Further subtleties associated with *m* are described in connection with the perturbations discussed in Section 4.

Let us now return to the free-rotor energy levels of Eq. [4]. For the case of fixed $K = 0$ and $m = 0, \pm 1, \pm 2, \cdots$ we obtain the simple Fm^2 energy level pattern of a particle on a ring, but it is actually more instructive for the general case to consider the energy levels of Eq. [4] as a function of *K* for fixed *m*. If levels for given positive *m* are plotted against the

TABLE 1

Correlation between the Torsional Quantum Number v_t^a and the Free-Rotor Quantum Number m^b for Levels of G_6 Symmetry Species $\Gamma = A$ or E^c

v_t	Γ	m	v_t	Γ	m	v_t	Γ	m	v_t	Γ	m	v_t	Γ	m
0	A_1	0	2	A_1	3	4	A_1	6	6	A_1	9	8	A_1	12
0	E	1	2	E	4	4	E	7	6	E	10	8	E	13
1	E	2	3	E	5	5	E	8	7	E	11	9	E	14
1	A_2	3	3	A_2	6	5	A_2	9	7	A_2	12	9	A_2	15

[a] Below the barrier the integer vibrational quantum number v_t gives the number of nodes of the vibrational eigenfunction occurring between the two classical turning points in one of the three equivalent torsional wells.
[b] The integer m is an internal rotation quantum number, taken to be positive in this table; 2m gives the number of nodes of the real free-rotor wavefunctions $\cos m\gamma$ and $\sin m\gamma$ in the interval $0 \le \gamma < 2\pi$.
[c] E states are doubly degenerate, with wavefunctions in the free-rotor limit of the form $e^{\pm im\gamma}$, $m \neq 0 \bmod 3$. The torsionally split A_1,A_2 pairs, with wavefunctions of the general form $\cos 3k\gamma$, $\sin 3k\gamma$, respectively, for integer $k > 0$, become one $e^{\pm i3k\gamma}$ doubly degenerate state in the free-rotor limit.

signed value of K they form a parabola with minimum at $K = -mF\rho/[A - (B + C)/2 + F\rho^2]$. The energy levels in Fig. 1 with $v_t \geqslant 3$ and $-10 \leqslant K \leqslant 10$ have been replotted in Fig. 2 and connected together in a way which illustrates this parabolic behavior. Note, however, that this zero-barrier limiting-case discussion gives only *qualitative* insight into the acetaldehyde levels in Fig. 2, since the 300 cm^{-1} free-rotor contribution to energies in the region of interest near $v_t = 3$ and 4 is comparable to the 400 cm^{-1} barrier contribution for this molecule, and both effects should be considered simultaneously. Two consequences of the nonzero barrier in acetaldehyde can easily be seen in Fig. 2; namely, the minima of the parabolas do not occur at the free-rotor K values determined from Eq. [4], and the doubly degenerate free-rotor level with $m = \pm 6$ and $K = 0$ in Eq. [4] is split by about 15 cm^{-1}. Note also, to avoid future notational confusion, that positive and negative values of K in Fig. 2 indicate that the pair of quantum numbers K and m have the same or opposite sign, respectively, whereas the traditional $+K$, $-K$ labels indicate that K and $m \bmod 3 \equiv \sigma = 0, +1, -1$ (from Eq. [3]) have the same or opposite sign.

A somewhat more quantitative understanding of the levels in Fig. 2 can be obtained by adding second-order perturbation corrections $E^{(2)}(m, K)$ arising from the nonzero barrier term $(1/2)V_3(1 - \cos 3\gamma)$ to the free rotor energies $E(m, K)$ of Eq. [4], where

$$\begin{aligned} E^{(2)}(m, K) &= V_3/2 + (V_3/4)^2/[F(m + \rho K)^2 - F(m + 3 + \rho K)^2] \\ &\quad + (V_3/4)^2/[F(m + \rho K)^2 - F(m - 3 + \rho K)^2] \\ &= V_3/2 + 18(V_3/4)^2/F[36(m + \rho K)^2 - 81]. \end{aligned} \quad [5]$$

This perturbation treatment of the internal rotation problem will diverge when the first-order mixing coefficient $V_{ij}/\Delta E_{ij}$ has a magnitude greater than unity, i.e., will diverge for the infinite number of m, K pairs satisfying (for either of the two sign choices)

$$|V_3/4F[9 \pm 6(m + \rho K)]| \geqslant 1. \quad [6]$$

Let us now examine in detail the applicability of this perturbation treatment to torsional levels above the barrier in acetaldehyde, characterized by the molecular constants $F \approx 7.6$ cm^{-1}, $V_3 \approx 408$ cm^{-1}, $\rho \approx 1/3$ and free-rotor m values satisfying $m \geqslant 5$. The Hamiltonian matrix for this problem, when set up using the basis functions $e^{+im\gamma} \equiv e^{+i(3k+\sigma)\gamma}$ generated by all positive and negative integer k values, has values of $F(3k + \sigma + \rho K)^2 + V_3/2$ on the diagonal, values of $-V_3/4$ everywhere on the first upper and first lower off-diagonal, and zero elsewhere. If $\rho \equiv 1/3$, this infinite matrix is invariant to the simultaneous transformation $K \to K \pm 3$ and $\sigma \to \sigma \mp 1 \bmod 3$, so that eigenvalues of the two $\sigma = 0$ energy matrices for $K = 0$ and 1 and the three $\sigma = +1$ matrices for $K = 0$, $+1$ and -1 are sufficient to generate eigenvalues (i.e., numerical energy levels) for all other K, σ pairs. (Mathematically, the torsional problem under discussion gives rise to only five distinct Hamiltonian matrices, and all K, σ pairs belonging to the same value of $|(3\sigma + K) \bmod 9| = 0, 1, 2, 3,$ or 4 yield the same matrix.) It is thus sufficient to examine the validity of the perturbation expression in Eq. [5] for $m \geqslant 5$ (i.e., above the barrier), and for the five $K = 0, \pm 1$ matrices. The ratio on the left of Eq. [6] for these five matrices varies from 0.32 to 0.71 for $m = 5$, from 0.29 to 0.54 for $m = 6$, and from 0.25 to

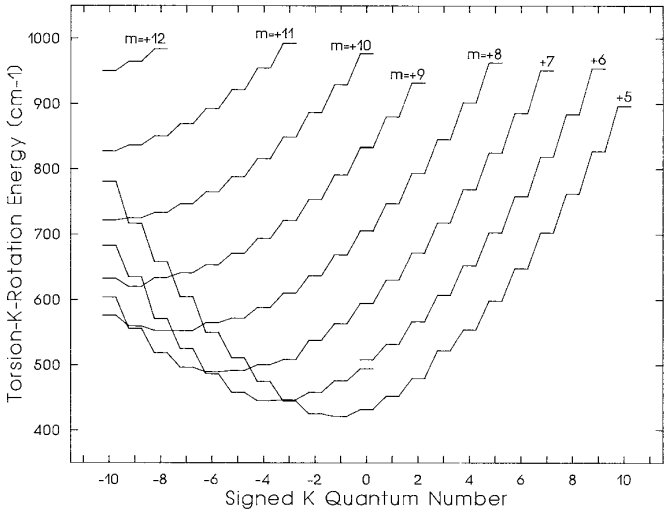

FIG. 2. An expanded representation of those levels in Fig. 1 having torsional energy contributions larger than the barrier height. Such levels, corresponding to $v_t \geqslant 3$ in acetaldehyde, are labeled here by a positive free-rotor quantum number m (see Table 1 for the correlation between v_t and m) and are plotted against a signed value of K. Note that the signed value of K is a rigorously good quantum number for the Hamiltonian in Eq. [1], whereas v_t and m are only approximate quantum numbers. (The integer m is closely related to the rigorous symmetry species, however, since torsion–K-rotation levels with $m = 0$ mod 3 are of A species and those with $m \neq 0$ mod 3 are of E species in the subgroup C_3 of C_{3v} which leaves H_{tKr} in Eq. [1] invariant.) When levels above the barrier are displayed as in this figure, they lie on parabolas with minima distributed along the K axis. Furthermore, on the energy scale of this figure, all levels are actually doubly degenerate, containing a partner with the sign of both m and K reversed, except for the $K = 0$, $m = 6$ level, which is clearly split into two (nondegenerate) components.

0.43 for $m = 7$, suggesting that the perturbation treatment for $K = 0$ and ± 1 will not diverge for $m \geqslant 5$.

Table 2 compares energy levels obtained from the second-order perturbation treatment with those obtained from the full torsion-K-rotation calculation, corresponding to the parabolas shown in Fig. 2. Agreement is quite good, although the $m = 6$ levels are not split in the second order treatment and comparison there must be made with the center of gravity of the $v_t = 3$, A_2 and the $v_t = 4$, A_1 torsional levels. Note also that even though the numerical energies in Table 2 obtained for $K = 0$ and 1 by the perturbation treatment can be transferred to other K levels by using the transformation $K \rightarrow K \pm 3$, $m \rightarrow m \mp 1$ (because of the high ''symmetry'' imposed on the problem by setting $\rho \equiv 1/3$), the perturbation treatment itself will often be inapplicable for these K values because of convergence difficulties.

The parabolas of Fig. 2 are shown in Fig. 3 plotted against $|K|$, which effectively folds the negative K parts of the parabolas over onto the positive K axis, and reproduces exactly (apart from scale expansions) the upper part of Fig. 1. Figure 3 can be understood by considering a plot of energy levels from Eq. [4] with $K \geqslant 0$ and m taken as a signed quantity (as shown in the figure). Figure 3 is particularly useful for discussing $\Delta K = 0$, $\Delta m = 0$ mod 3 interactions. Such interactions, as discussed in more detail in Section 4B, arise from matrix elements of the torsional barrier, which were neglected in deriving Eq. [4] and which lead to irregular energy spacings in the regions where two parabolas with the same m mod 3 cross. Five such large avoided crossings are circled in the acetaldehyde levels of Fig. 3. Four of these avoided crossings are also present in Fig. 2, but they correspond to pairs of levels labeled there as $K = 0$, $m = 6$; $K = +3$, $m = 5$ and $K = -3$, $m = 7$; $K = -6$, $m = 5$, 8; and $K = -9$, $m = 6$, 9.

The occurrence of avoided crossings indicates that energy level connections as drawn in Figs. 2 and 3 will sometimes be misleading, i.e., when barrier effects are large compared to free rotor energies it is in fact more appropriate to draw

TABLE 2

Comparison of Torsion–K-Rotation Energies (in cm^{-1}) Obtained from a Large Basis Set Matrix Diagonalization with Free-Rotor Torsion–K-Rotation Energies Corrected to Second Order for Barrier Effects

m,K	E_{diag}[a]	E_{pert}[b]	m,K	E_{diag}[a]	E_{pert}[b]	m,K	E_{diag}[a]	E_{pert}[b]
5,0	431.5	425.4	5,1	450.4	447.5	5,-1	419.4	405.8
6,0	501.0[c]	499.9	6,1	530.4	528.8	6,-1	474.0	473.0
7,0	594.4	593.9	7,1	629.0	628.7	7,-1	561.8	561.0
8,0	705.5	705.2	8,1	745.7	745.5	8,-1	667.0	666.7

[a] Torsion-K-rotation energies obtained by diagonalization of a 21x21 matrix representation of H_{tor}(F=7.66 cm^{-1}, V_3=408 cm^{-1}, ρ=0.3291) in Eq. (1). These levels are shown in Fig. 4.

[b] Second-order perturbation energies from the sum of Eqs. (4) and (5), after subtraction of $[A-(B+C)/2]K^2$.

[c] Average of the two split levels at 494.05 and 507.94 cm^{-1}.

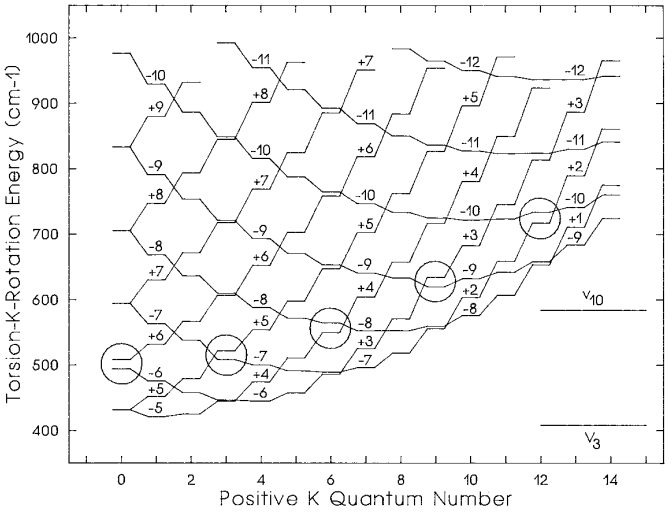

FIG. 3. An alternative representation of Fig. 2, in which levels are plotted against positive values of K and labeled by signed values of m. The different m values at various K positions indicate the dominant free-rotor basis set function in the actual torsion–K-rotation eigenfunction at that K value; for levels exhibiting an energy minimum in this figure this m value changes by 9 units shortly after the minimum. Avoided crossings occur in this figure between levels satisfying $\Delta K = 0$ and $\Delta m = 0$ mod 3; the five largest of these (satisfying $\Delta m = 12$) are circled. Avoided crossings satisfying $\Delta m = 18$ also occur, but the mutual interactions are much smaller, and ''splittings'' at these crossings arise mainly because $\rho - 1/3 \neq 0$. The top of the barrier V_3 and the lowest small-amplitude vibrational mode ν_{10} (after addition of 75 cm^{-1} of torsional zero-point energy) are indicated by the two horizontal lines at the right of this figure. Torsion–K-rotation levels studied in the present work lie between these two energies.

level connections which obey the noncrossing rule. Thus, in Fig. 4 the $v_t \geqslant 3$ energy levels of Fig. 1 with $[A - (B + C)/2]K^2$ subtracted are replotted, and levels of the same symmetry (same m mod 3) are connected together in a way which illustrates the periodic nature of the ''torsional splittings'' for given v_t required by the cosine series in Eq. [3]. Since ρ is quite close to 1/3 for acetaldehyde, splitting patterns in Fig. 4 essentially repeat with a periodicity of 9 in the quantum number K. Note that the v_t, K and symmetry labels used in our fitting program, and therefore also in the tables of this paper, correspond to those shown in Fig. 4.

3. SPECTRAL ANALYSIS OF TRANSITIONS INVOLVING $v_t = 3$ AND 4

A. Data Set

The data set previously treated (*1–5*) has been extended to include (i) millimeter-wave measurements of *b*-type transitions in $v_t = 2$, which fix much more precisely $\Delta K \neq 0$ intervals in this last state below the barrier to internal rotation in acetaldehyde; (ii) microwave and far-infrared transitions involving $v_t = 3$, the first torsional state above the barrier, up to the point where torsion-rotation levels of $v_t = 3$ begin to interact with the lowest small-amplitude vibrational mode ν_{10}; (iii) a few microwave transitions involving the nine torsion–K-rotation levels of $v_t = 4$ which lie below ν_{10} (see Fig. 3); and (iv) a number of remeasurements at higher accuracy of lines in the previous data set. These measurements come from a variety of sources, which can be summarized separately for $v_t \leqslant 2$ and $v_t \geqslant 3$ as follows.

Previous $v_t \leqslant 2$ millimeter-wave measurements from Nizhny Novgorod came from the RAD-3 spectrometer (*8, 9*), with a frequency range of 165–417 GHz and a measurement precision better than 1 MHz. Since it was difficult to identify the weak *b*-type lines in this spectrum with certainty, the previous fit (*5*) contained information on $\Delta K \neq 0$ intervals in the $v_t = 2$ state only from far-infrared transitions, i.e., only to an accuracy of about ±15 MHz. The new measurements (mainly in $v_t = 2$) from the RAD-2 spectrometer (*10*) provided about 90 *b*-type lines in the range from 179 to 380 GHz with measurement precision better than the 70 kHz uncertainty assigned in our global fit. In addition to these new *b*-type lines, about 275 *a*-type lines were measured or remeasured with RAD-2 to permit precise combination difference verification of a number of *b*-type assignments. (Note that here and elsewhere, frequencies for unresolved

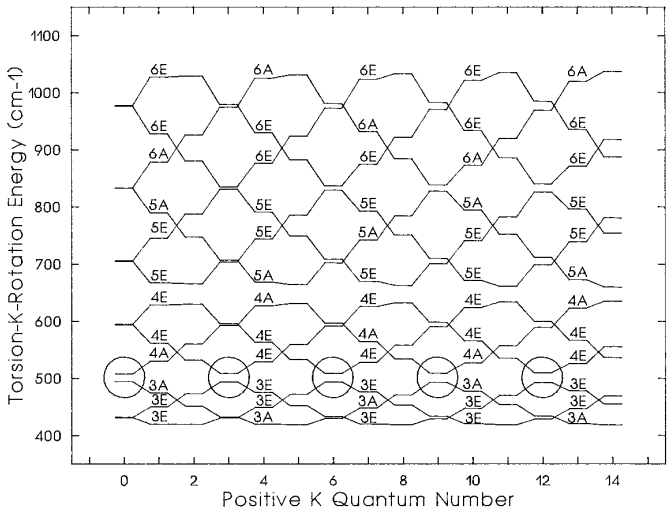

FIG. 4. Energy levels above the barrier from Fig. 1, plotted against positive K after $[A - (B + C)/2]K^2$ has been subtracted, in order to better illustrate the approximate periodicity (every 9 units in K) of the torsional splittings; lack of perfect periodicity arises because the value of ρ is not exactly 1/3. Torsional levels in this figure correspond closely to the torsion–K-rotation levels in Fig. 3, but levels here are labeled by the torsional vibrational quantum number v_t (not a good quantum number) and the A or E torsional symmetry species, instead of by the free-rotor quantum number m (also not a good quantum number). The five $\Delta K = 0$, $\Delta m = 12$ avoided crossings circled in Fig. 3 are also circled here. The v_t, K and A, E symmetry labels in this figure are the same as those used in our fitting program and in Tables 4–6 here. Levels of E species in these tables with positive and negative values of K_a correspond to levels in Fig. 3 with m mod 3 = +1 and −1, respectively.

doublets are counted as two lines when they appear twice in the data set.)

About 40 $v_t = 2$ lines in the region from 53–72 GHz were newly measured or remeasured at NIST, with an accuracy of 70 kHz. In addition, the rather important $v_t = 0$ $J = 1 \leftarrow 0$ A line, which was previously measured with the Fourier transform instrument at NIST at 19 265.096(4) MHz (*2*) and which was excluded from previous fits because of its large observed minus calculated value, was remeasured (*11*); the new value of 19 265.133(4) MHz now fits within experimental accuracy.

The millimeter-wave spectrometer at Lille (*12*) provided about 30 new measurements or remeasurements of $v_t = 0$, 1, and 2 lines in the region from 153 to 318 GHz, again with measurement precision better than the ±70 kHz assigned in our global fits.

A number of far infrared $v_t = 2 - 1$ E species subbands involving K values of −7, −8, and −9 were added to the fit after reexamination of the Ottawa BOMEM spectrum (*1*).

About 250 a-type millimeter-wave $v_t = 3$ lines and 27 a-type $v_t = 4$ lines were assigned by reexamination of the RAD-3 spectrum from Nizhny Novgorod. These lines are in the frequency range from 165 to 417 GHz and in the rotational quantum number range from $7 \leqslant J \leqslant 22$, with measurement precision better than the ±1 MHz uncertainty assigned in our global fit. In addition, about 35 $v_t = 3$ lines and 12 $v_t = 4$ lines were measured at NIST (with uncertainties of 180 kHz), about 40 $v_t = 3$ lines and three $v_t = 4$ lines were measured at Lille, and eight other $v_t = 3$ and 4 lines were found in the literature (*13*).

Finally, 224 far-infrared $v_t = 3 - 2$ hot band transitions were assigned by reexamination of the Ottawa BOMEM spectrum (*1*). Unfortunately, a number of subbranches belonging to this hot band either fall outside the range of the spectral recording (i.e., below 80 cm^{-1}) or are overlapped by the lower $v_t = 2 - 1$ and $1 - 0$ bands in this sequence.

B. Experimental Details

Instruments and experimental conditions involved in the new measurements are described briefly below.

The Nizhny Novgorod RAD-2 lines were measured using a BWO-based frequency synthesizer and acoustic detector cell as described in the review by Krupnov (*10*). Frequency measurements were carried out according to the methods described in Ref. (*14*), using 180 Hz frequency-modulated synthesizer radiation, which was stabilized against a 30 MHz reference synthesizer generator by four phase-locked loops and then locked to the line center with an approximately 1 sec time constant. Because the pressure self-broadening line parameter for acetaldehyde is quite large and the spectrum is quite dense, it was necessary to change our customary operating conditions somewhat. Reducing the pressure to 20–40 mTorr gave acceptable resolution, but led to a considerable loss in sensitivity of the acoustic detector. Argon, chosen for its small pressure broadening effects on the acetaldehyde spectrum, was thus added as a buffer gas to the acetaldehyde sample in about a 5 to 1 ratio in order to bring the final total static pressure in the cell to about 0.2 Torr. This arrangement led to a satisfactory balance between signal-to-noise and resolution, i.e., to an estimated sensitivity of about 10^{-7} cm^{-1} and a measurement uncertainty of about 50 kHz.

A number of new measurements were made using several setups at NIST. A 1 m glass cell with Stark electrodes was used together with various OKI klystrons to test early predictions for $v_t = 3$ transitions in the region 43 to 74 GHz. Later a conventional 1.1 m waveguide equipped with a Stark septum as sample cell and a Hewlett–Packard synthesizer and frequency doubler as radiation source was used in the range 32–40 GHz. Finally, a 0.3 m parallel plate cell and a KVARTZ synthesizer with two BWO source modules were used in their fundamental regions of 53–78 and 78–118 GHz, or in a frequency-doubled mode. Millitek mm-wave detectors were used in the ranges above 53 GHz. Because sample cells in all cases were somewhat shorter than optimum length, uncertainties for these measurements of weak $v_t > 0$ lines are somewhat larger than normal.

Millimeter-wave measurements were carried out at Lille (*12*) using a computer controlled spectrometer and harmonics of a Gunn diode (74–80 GHz) as sources and a He-cooled bolometer as a detector. These frequency measurements have an estimated uncertainty of about 70 kHz.

C. Theoretical Model for the Spectral Fit

The theoretical model and computer program used in this study is the same as those used in our previous papers (*1–5*), and is based on the work of Refs. (*15, 16*). Two changes were made, however. First, the size of the torsional basis set retained after diagonalization of the purely torsional Hamiltonian (*1–3, 15, 16*) was increased from seven functions to nine. This was necessary to achieve sufficient accuracy in calculated levels for $v_t = 3$ and 4. Second, about 20 new terms were added to the Hamiltonian operator to allow for higher order rotation–torsion interactions.

D. Global Fits

A relatively satisfactory global fit of the data set described in Section 3A was obtained using 55 adjustable and 2 fixed parameters. (Attempts to set the fixed parameters to zero resulted in significant deterioration of the fits.) Values for the fixed and adjustable parameters, as well as expressions for the corresponding operators they multiply in our program, are given in Table 3 in the notation of Ref. (*5*). The number of parameters used, though large, is still considerably less than the 89 parameters (i.e., three rotational constants and five centrifugal distortion constants for each of the 10 torsion–vibration levels plus nine ν_0 values) which

TABLE 3

The 57 Torsion–Rotation Parameters Used in the Present Global Fit of Transitions Involving Levels of the v_t = 0, 1, 2, 3, and 4 Torsional States of Acetaldehyde together with a Comparison with Parameters from a Fit of v_t = 0, 1, and 2 Data

nℓm[a]	Operator[b]	Parameter[b]	($v_t \le 2$)[c]	($v_t \le 4$)[d]	nℓm[a]	Operator[b]	Parameter[b]	($v_t \le 2$)[c]	($v_t \le 4$)[d]
220	$(1/2)(1-\cos 3\gamma)$	V_3	407.947(2)	407.716(10)	660	$(1/2)(1-\cos 9\gamma)$	V_9	not used	-0.186(2)
	P_γ^2	F	7.6559(6)	7.5997(28)		P_γ^6	k_{4B}	not used	$-0.820(4)\times10^{-6}$
211	$P_\gamma P_a$	ρ	0.3291(2)	0.3316(1)	651	$P_\gamma^5 P_a$	k_{3B}	not used	$-0.119(1)\times10^{-5}$
202	P_a^2	A	1.8848741(9)	1.8851594(68)	642	$(1-\cos 6\gamma)P^2$	N_v	$0.479(2)\times10^{-4}$	$0.554(1)\times10^{-4}$
	P_b^2	B	0.3487163(5)	0.3487056(3)		$(1-\cos 6\gamma)P_a^2$	K_2	$-0.279(4)\times10^{-3}$	$0.395(20)\times10^{-3}$
	P_c^2	C	0.3031777(1)	0.30318096(4)		$P_\gamma^4 P_a^2$	K_1	not used	$-0.56(1)\times10^{-6}$
	$(P_aP_b+P_bP_a)$	D_{ab}	-0.122709(3)	-0.122636(2)		$P_\gamma^4 P^2$	M_v	$0.2(1)\times10^{-8}$	not used
440	$(1/2)(1-\cos 6\gamma)$	V_6	-12.918(8)	-12.068(37)		$2P_\gamma^4(P_b^2-P_c^2)$	c_3	$-0.15(6)\times10^{-8}$	$0.29(1)\times10^{-8}$
	P_γ^4	k_4	$-0.4313(2)\times10^{-3}$	$-0.4384(2)\times10^{-3}$		$\{(1-\cos 3\gamma),P_\gamma^2\}P_a^2$	k_{7K}	not used	$0.64(2)\times10^{-4}$
	$\{(1-\cos 3\gamma),P_\gamma^2\}$	k_7	-0.0445(3)	-0.0163(14)		$(1-\cos 6\gamma)(P_aP_b+P_bP_a)$	dd_{ab}	not used	$-0.705(7)\times10^{-4}$
431	$P_\gamma^3 P_a$	k_3	$-0.8363(4)\times10^{-3}$	$-0.8509(3)\times10^{-3}$	633	$P_\gamma^3 P_a P^2$	k_{3J}	$-0.22(2)\times10^{-7}$	$-0.59(2)\times10^{-8}$
	$\{(1-\cos 3\gamma),P_\gamma P_a\}$	k_6	-0.033(2)	-0.033511565[e]		$\{(1-\cos 3\gamma),P_\gamma P_a^3\}$	k_{6K}	not used	0.5677008×10^{-4}[e]
422	$P_\gamma^2 P^2$	G_v	$-0.284(3)\times10^{-5}$	$-0.2966(2)\times10^{-5}$	624	$P_\gamma^2 P^4$	g_v	$0.5(1)\times10^{-10}$	not used
	$P_\gamma^2 P_a^2$	k_2	$-0.9838(6)\times10^{-3}$	$-1.1162(32)\times10^{-3}$		$P_\gamma^2 P_a^2 P^2$	k_{2J}	$-0.25(1)\times10^{-7}$	$-0.074(1)\times10^{-7}$
	$2P_\gamma^2(P_b^2-P_c^2)$	c_1	$-0.142(3)\times10^{-5}$	$-0.405(4)\times10^{-5}$		$P_\gamma^2 P_a^4$	k_{2K}	$0.87(4)\times10^{-7}$	$1.62(3)\times10^{-7}$
	$P_\gamma^2(P_aP_b+P_bP_a)$	Δ_{ab}	$0.42(1)\times10^{-4}$	$0.401(3)\times10^{-4}$		$(1-\cos 3\gamma)(P_b^2-P_c^2)P^2$	c_{2J}	not used	$-0.44(1)10^{-8}$
	$\sin 3\gamma(P_aP_c+P_cP_a)$	D_{ac}	$-0.14(1)\times10^{-2}$	$-0.185(4)\times10^{-2}$		$2P_\gamma^2(P_b^2-P_c^2)P^2$	c_{1J}	$-0.95(5)\times10^{-10}$	$0.29(4)\times10^{-10}$
	$\sin 3\gamma(P_bP_c+P_cP_b)$	D_{bc}	not used	$-0.341(5)\times10^{-3}$		$(1-\cos 3\gamma)P^4$	f_v	$-0.87(3)\times10^{-8}$	$-0.722(5)\times10^{-8}$
	$(1-\cos 3\gamma)P^2$	F_v	$0.5587(4)\times10^{-3}$	$0.55891(6)\times10^{-3}$		$(1-\cos 3\gamma)P_a^2P^2$	k_{5J}	$0.28(9)\times10^{-7}$	not used
	$(1-\cos 3\gamma)P_a^2$	k_5	-0.031(1)	-0.0380(3)		$(1-\cos 3\gamma)P_a^4$	f_k	$0.80(9)\times10^{-6}$	$24.6(3)\times10^{-6}$
	$(1-\cos 3\gamma)(P_b^2-P_c^2)$	c_2	$0.2053(5)\times10^{-3}$	$0.20878(8)\times10^{-3}$	615	$P_\gamma P_a P^4$	ℓ_v	not used	$0.18(2)\times10^{-10}$
	$(1-\cos 3\gamma)(P_aP_b+P_bP_a)$	d_{ab}	$0.2103(3)\times10^{-2}$	$0.20996(6)\times10^{-2}$		$P_\gamma P_a^5$	ℓ_k	$0.67(3)\times10^{-7}$	$0.86(1)\times10^{-7}$
413	$P_\gamma P_a P^2$	L_v	$0.60(1)\times10^{-5}$	$0.578(2)\times10^{-5}$		$P_\gamma P_a^3 P^2$	λ_v	$-0.113(4)\times10^{-7}$	$-0.0544(6)\times10^{-7}$
	$P_\gamma P_a^3$	k_1	$-0.5596(3)\times10^{-3}$	$-0.6753(1)\times10^{-3}$	606	$P_a^4P^2$	H_{KJ}	$-0.198(8)\times10^{-8}$	$-0.144(1)\times10^{-8}$
	$P_\gamma\{P_a,(P_b^2-P_c^2)\}$	c_4	$-0.429(8)\times10^{-5}$	$-0.526(3)\times10^{-5}$		P_a^6	H_K	$0.113(7)\times10^{-7}$	$0.149(3)\times10^{-7}$
	$P_\gamma(P_a^2P_b+P_bP_a^2)$	δ_{ab}	$0.60(2)\times10^{-4}$	$0.450(4)\times10^{-4}$	880	$(1/2)(1-\cos 12\gamma)$	V_{12}	not used	0.1076(2)
404	$-P^4$	Δ_J	$0.3212(3)\times10^{-6}$	$0.3119(1)\times10^{-6}$	1082	$(1-\cos 12\gamma)P^2$	V_{12J}	not used	$-0.191(4)\times10^{-5}$
	$-P^2P_a^2$	Δ_{JK}	$-0.28(1)\times10^{-5}$	$-0.442(2)\times10^{-5}$					
	$-P_a^4$	Δ_K	$0.1246(2)\times10^{-3}$	$0.1518(4)\times10^{-3}$					
	$-2P^2(P_b^2-P_c^2)$	δ_J	$0.750(1)\times10^{-7}$	$0.7068(5)\times10^{-7}$					
	$-\{P_a^2,(P_b^2-P_c^2)\}$	δ_K	$0.223(5)\times10^{-5}$	$0.1306(8)\times10^{-5}$					
	$(P_aP_b+P_bP_a)P^2$	D_{abJ}	$0.886(6)\times10^{-6}$	$0.670(2)\times10^{-6}$					
	$(P_a^3P_b+P_bP_a^3)$	D_{abK}	$0.213(7)\times10^{-4}$	$0.103(1)\times10^{-4}$					

[a]Notation of Ref. (17): n ≡ ℓ+m, where n is the total order of the operator, ℓ is the order of the torsional part and m is the order of the rotational part, respectively.
[b]Notation of Refs. (15,16). {A,B} ≡ AB+BA. The product of the parameter and operator from a given row yields the term actually used in the vibration-rotation-torsion Hamiltonian, except for F, ρ and A, which occur in the Hamiltonian in the form $F(P_\gamma+\rho P_a)^2 + AP_a^2$.
[c]Values of the parameters from the fit in Ref. (5).
[d]Values of the parameters from the fit shown in Tables III-VII. All values are in cm^{-1}, except for ρ, which is unitless. Uncertainties are shown as one standard deviation in the last digit(s).
[e]These two parameters were fixed in the $v_t \le 4$ fit.

might be used in a separate band-by-band analysis of the *A* and *E* components of v_t = 0, 1, 2, 3, and 4 torsional states.

Table 4 gives assignments, observed frequencies, and observed minus calculated values from the global fit for the v_t = 0–0, 1–1, and 2–2 microwave measurements or remeasurements. Tables 5 and 6 give similar information for the v_t = 3–3 and 4–4 microwave transitions and for the v_t = 3–2 far-infrared transitions, respectively. An overview of

TABLE 4

Assignments,[a] Observed Values,[b] Residuals from the Fit[c] and Sources[d] for Remeasured Microwave Transitions within the v_t = 0, 1, and 2 States

v_tJ'K_a'K_c'P'	J"K_a"K_c"P"	Frequency	O-C	Lit
2 3 2 1 +	2 2 0 -	53174.426(70)	0.102	Q
2 16 2 14 +	16 1 15 -	53337.918(70)	0.091	Q
2 9 1 8 -	9 1 9 +	53356.692(70)	0.106	Q
2 15 2 13 +	15 1 14 -	53877.562(70)	-0.022	Q
2 5 -1 5 -	5 -2 4 +	54448.944(70)	0.404	Q
2 19 3 16 -	20 2 19 -	55654.344(70)	0.067	Q
2 6 -2 5 -	5 -1 5 +	56002.230(70)	-0.247	Q
2 3 1 3 +	2 1 2 +	56555.700(70)	-0.014	Q
2 20 3 17 +	20 2 18 -	56773.420(70)	0.114	Q
2 19 2 17 +	19 2 18 -	56956.190(70)	0.002	Q
2 17 2 15 +	17 1 16 -	57020.338(70)	0.023	Q
2 3 1 2 +	2 1 1 -	57731.496(70)	0.188	Q
2 14 2 12 +	14 1 13 -	57920.412(70)	-0.021	Q
2 3 2 2 -	2 2 1 -	58261.120(70)	0.086	Q
2 3 2 1 +	2 2 0 +	58303.895(70)	-0.028	Q
2 3 0 3 +	2 0 2 +	58323.040(70)	-0.008	Q
2 3 0 3 -	2 0 2 -	59222.453	-0.679 *	Q
2 9 2 8 -	10 1 9 -	59307.434(70)	-0.012	Q
2 16 -1 16 -	16 -2 15 -	59877.220(70)	-0.122	Q
2 3 1 2 -	2 1 1 -	60119.078(70)	0.032	Q
2 6 -1 6 -	6 -2 5 -	61269.568(70)	0.343	Q
2 6 1 5 -	7 0 7 -	62226.056	0.160 *	Q
2 3 2 1 +	4 1 3 +	62238.585(70)	0.136	Q
2 3 -1 3 -	2 -1 2 -	62680.650(70)	-0.050	Q
2 15 -1 15 -	15 -2 14 -	63815.840(70)	-0.085	Q
2 13 2 11 +	13 1 12 -	64248.184(70)	-0.011	Q
2 18 2 16 +	18 1 17 -	64542.208(70)	0.055	Q
2 10 1 9 -	10 1 10 +	65163.632(70)	0.113	Q
2 16 3 14 +	17 2 15 +	66396.160(70)	-0.010	Q
2 7 -1 7 -	7 -2 6 -	66580.960(70)	0.273	Q
2 14 -1 14 -	14 -2 13 -	67301.700(70)	0.005	Q
2 19 3 16 +	19 2 17 -	67495.776(70)	-0.028	Q
2 9 2 7 +	8 3 5 -	67724.985(70)	-0.026	Q
2 20 2 18 +	20 2 19 -	68059.461(70)	0.049	Q
2 7 -2 6 -	6 -1 6 -	68705.769(70)	-0.209	Q
2 9 1 8 -	8 2 6 -	69134.752(70)	-0.017	Q
2 3 0 3 +	4 -1 4 -	70176.240(70)	-0.191	Q
2 13 -1 13 -	13 -2 12 -	70189.920(70)	0.044	Q
2 8 -1 8 -	8 -2 7 -	70384.064(70)	0.190	Q
2 8 0 8 +	7 1 7 +	71100.976(70)	-0.030	Q
2 4 -2 3 -	3 -2 2 -	71355.864(70)	0.117	Q
2 4 2 2 -	3 2 1 -	71395.740(70)	0.068	Q
2 12 2 10 -	12 1 11 -	71819.360(70)	0.003	Q
2 18 3 15 -	19 2 18 -	71977.912(70)	0.014	Q
2 12 -1 12 -	12 -2 11 -	72330.800(70)	0.037	Q
0 6 2 5 -	6 1 6 +	153004.351(70)	0.075	V
1 19 -2 17 -	18 -3 15 -	159221.120(70)	-0.290	V
1 19 3 16 -	19 2 17 +	178683.770(70)	0.001	M
2 9 1 8 -	8 1 7 -	180019.869(70)	0.031	M
0 26 3 23 -	26 2 24 +	180259.537(70)	0.286	M
2 9 0 9	8 0 8	181480.471(70)	0.104	M
2 2 2 0	1 1 0	182278.271(70)	0.073	M
2 5 2 3 +	6 1 6 +	182676.093(70)	0.155	M
0 22 3 19 -	22 2 20	182843.354(70)	-0.154	M
2 10 5 5 -	9 5 4 -	186193.361(70)	-0.060	M
2 10 5 6 +	9 5 5 +	186193.361(70)	-0.058	M
2 15 1 14 -	15 0 15 +	187096.949(70)	0.171	M
2 5 1 5 +	4 0 4 +	187744.198(70)	0.200	M
2 10 1 10 +	9 1 9 +	188110.856(70)	0.008	M
2 10 -9 1 -	9 -9 0 -	188126.359(70)	0.152	M
2 10 -2 9 -	9 -2 8 -	188352.838(70)	-0.002	M
0 19 1 18 -	19 -1 19 -	188424.090	0.993 *	M
2 13 0 13 +	12 1 12 +	188452.432(70)	0.024	M
2 10 6 4 +	9 6 3 +	189021.376(70)	0.003	M
2 10 6 5 -	9 6 4 -	189021.376(70)	0.003	M
2 19 1 18 -	18 2 17 -	189343.673(70)	0.124	M
2 10 -1 10 -	9 -1 9 -	189369.889(70)	-0.212	M
2 10 0 10 -	10 -1 10 -	189755.167(70)	-0.111	M
2 10 -7 3 -	9 -7 2 -	190005.295(70)	-0.076	M
2 8 1 7 -	8 0 8 -	190395.385	-0.374 *	M
2 10 4 6 +	9 4 5 +	190683.211	-0.335 *	M
2 10 4 7 -	9 4 6 -	190683.211	0.283 *	M
2 10 -3 8 -	9 -3 7 -	192283.746(70)	-0.088	M
2 10 1 9 -	9 1 8 -	193363.618(70)	0.119	M
1 10 -8 3 -	9 -8 2 -	193373.987(70)	0.003	M
2 10 3 8 +	9 3 7 +	193560.248(70)	0.002	M
2 10 3 7 -	9 3 6 -	193611.805(70)	-0.022	M
2 10 -5 5 -	9 -5 4 -	194529.515(70)	-0.035	M
2 10 2 8 +	9 2 7 +	195639.373(70)	-0.024	M
2 7 1 6 -	7 0 7 -	197239.384	0.492 *	M
2 5 -3 3 -	5 -2 4 -	198648.034(70)	-0.277	M
2 10 5 6 -	9 5 5 -	198817.654(70)	0.166	M
2 10 1 9 -	9 1 8 -	199917.783(70)	0.002	M
2 16 1 15 -	16 0 16 +	200861.634(70)	0.069	M
1 17 2 16 -	17 1 17 +	201457.869	-0.501 *	M
2 10 0 10	9 0 9	201479.570(70)	0.094	M
2 6 1 5 -	6 0 6	203130.455	0.239 *	M
2 11 0 11	11 -1 11	203452.462(70)	-0.239	M
2 6 1 6 +	5 0 5 +	203721.436(70)	0.104	M
2 6 -3 4 -	6 -2 5	204185.218(70)	-0.163	M
2 11 -8 3 -	10 -8 2	204226.585(70)	-0.189	M
2 11 2 9 -	10 2 8	204535.897(70)	0.046	M
1 8 -2 6 -	8 1 8	205669.015(70)	0.028	M
2 14 1 13 -	13 2 11	206584.615(70)	0.161	M
2 11 3 8 -	10 3 7	206716.667	-0.224 *	M
2 11 1 11 +	10 1 10 +	206824.538(70)	0.019	M
2 11 -9 2 -	10 -9 1 -	206892.847(70)	0.208	M
2 11 -1 11 -	10 -1 10 -	207518.307(70)	0.001	M
2 11 -2 10 -	10 -2 9 -	207704.698(70)	0.042	M
2 11 6 5 +	10 6 4 +	207902.590	0.827 *	M
2 11 6 6 -	10 6 5 -	207902.590	0.827 *	M
2 11 10 2 -	10 10 1 -	208476.649(70)	-0.181	M
2 11 -7 4 -	10 -7 3 -	209034.092(70)	-0.071	M
2 7 -3 5 -	7 -2 6 -	209293.048(70)	-0.245	M
2 11 4 7 +	10 4 6 +	209802.918	-0.642 *	M
2 11 4 8 -	10 4 7 -	209802.918	0.604 *	M
2 4 2 2	3 1 2	210640.926(70)	0.243	M
2 11 -3 9	10 -3 8	211360.620(70)	0.043	M
1 11 6 5	10 6 4	211667.691(70)	-0.012	M
2 11 -6 5	10 -6 4	212564.645(70)	0.030	M
2 11 1 10	10 1 9	212867.643(70)	0.080	M
2 11 3 9 +	10 3 8 +	212949.224(70)	0.123	M
2 11 3 8 -	10 3 7 -	213033.001(70)	-0.001	M
1 15 -1 14	14 2 13	213200.584(70)	-0.035	M
2 11 2 10 -	10 2 9 -	213213.358(70)	0.016	M
2 11-10 1	10-10 0	213379.461	0.422 *	M
2 11 -5 6	10 -5 5	214023.386(70)	-0.113	M
2 11 7 4 -	10 7 3 -	214160.451(70)	0.167	M
2 11 7 5 +	10 7 4 +	214160.451(70)	0.167	M
2 11 -4 8	10 -4 7	215309.218(70)	-0.089	M
2 11 7 5	10 7 4	215355.666(70)	-0.134	M
2 12 5 7 -	11 5 6 -	223986.729(70)	-0.071	M
2 12 5 8 +	11 5 7 +	223986.729(70)	-0.053	M
2 12 2 10	11 2 9	224203.636(70)	0.064	M
2 12 3 9	11 3 8	225512.043(70)	0.007	V
2 12 1 12 +	11 1 11 +	225513.218(70)	0.027	V
2 12 -9 3	11 -9 2	225629.937(70)	0.153	M
2 11 -3 9	11 -2 10	225842.993(70)	-0.191	M
2 12 6 6 +	11 6 5 +	226787.800(70)	0.014	M
2 12 6 7 -	11 6 6 -	226787.800(70)	0.015	M
0 11 3 8	11 2 9	226857.771(70)	0.057	V
2 12 -2 11	11 -2 10	226980.968(70)	-0.069	M
0 10 -3 8	10 2 8	227293.854(70)	-0.073	M
2 12 10 3	11 10 2	227437.461(70)	-0.247	M
2 12 4 9 -	11 4 8 -	228934.938(70)	0.043	V
2 12 4 8 +	11 4 7 +	228937.243	-0.008 *	V
2 12 -3 10	12 -2 11	229323.503(70)	-0.103	M
2 12 0 12 +	11 0 11 +	230438.326(70)	0.052	M
1 12 10 2 +	11 11 0	230757.071(70)	0.120	M
1 12 10 3 -	11 10 2 -	230757.071(70)	0.120	M
2 15 1 14	14 2 12	231570.317(70)	0.112	V
2 12 9 4	11 9 3	231904.051(70)	0.004	V
2 12 -6 6	11 -6 5	231908.022(70)	-0.039	V
2 12-10 2	11-10 1	232365.810(70)	0.324	M
2 12 2 11 -	11 2 10 -	232503.524(70)	-0.027	V
2 13 -3 11	13 -2 12	232750.985(70)	-0.102	V
2 12 7 5 -	11 7 4 -	233274.064(70)	0.047	M
2 12 7 6 +	11 7 5 +	233274.064(70)	0.047	M
2 12 -5 7	11 -5 6	233529.343(70)	-0.087	V
2 12 8 5	11 8 4	233745.416(70)	-0.003	M
2 13 0 13	13 -1 13	234097.624(70)	-0.087	V
2 12 11 1 -	11 11 0 -	234099.979(70)	0.044	V
2 12 11 2 +	11 11 1 +	234099.979(70)	0.044	V
2 19 2 17 +	19 1 18 -	234344.120(70)	-0.066	M
2 12 4 8	11 4 7	234708.018(70)	-0.036	V
2 12 7 6	11 7 5	234982.673(70)	-0.007	M
2 12 -4 9	11 -4 8	235044.190(70)	0.037	M
2 20 2 18 +	20 1 19 -	235278.021(70)	-0.075	M
2 12 10 2 +	11 10 1 +	235291.609(70)	-0.010	V
2 12 10 3 -	11 10 2 -	235291.609(70)	-0.010	V
2 17 2 15 +	17 1 16 -	235345.115(70)	-0.086	M
2 15 0 15 +	14 1 14 +	235357.594(70)	-0.002	M
2 12 2 10 +	11 2 9 +	235457.870(70)	-0.074	M
2 12-11 1	11-11 0	236012.353(70)	0.076	V
2 12 9 3 -	11 9 2 -	236205.941(70)	-0.006	M
2 12 9 4 +	11 9 3 +	236205.941(70)	-0.033	M
2 12 8 4 +	11 8 3 +	236251.579(70)	0.071	M
2 12 8 5 -	11 8 4 -	236251.579(70)	0.087	M
2 14 -3 12	14 -2 13	236268.507(70)	-0.031	M
2 12 6 7	11 6 6	236507.149(70)	0.265	M
2 16 2 14 +	16 1 15 -	237100.687(70)	-0.078	M
2 21 2 19 +	21 1 20 -	237274.536(70)	0.010	M
2 12 5 8	11 5 7	238406.583(70)	0.109	M
1 10 -3 7	10 -2 8	239353.561(70)	-0.079	V
2 15 2 13 +	15 1 14 -	239560.243(70)	-0.074	M
2 12 1 11 -	11 1 10 -	239601.046(70)	0.014	M
2 15 -3 13	15 -2 14	240035.212	0.166 *	M
2 12 0 12	11 0 11	240651.908	-0.249 *	M
2 9 -1 9	8 -2 7	241679.154(70)	0.180	M
2 13 5 8 -	12 5 7 -	242951.557(70)	-0.079	M
2 13 5 9 +	12 5 8 +	242951.557(70)	-0.039	M
2 13 -1 13	12 -1 12	244028.772	0.156 *	M
2 13 2 11	12 2 10	244147.005(70)	0.010	M
2 13 1 13 +	12 1 12 +	244175.819(70)	0.001	M
2 13 -9 4	12 -9 3	244313.086(70)	-0.086	M
2 13 3 10	12 3 9	244362.360(70)	0.015	M
2 9 1 9 +	8 0 8 +	248886.594(70)	0.076	M
2 17 -3 15	17 -2 16	248994.566(70)	0.053	M
0 16 3 14 +	16 2 15 -	249109.957(70)	0.043	M
2 13 0 13 +	12 0 12 +	249119.263(70)	0.034	M
2 13 -3 11	12 -3 10	249597.064(70)	0.080	M
2 14 0 14	14 -1 14	250257.901	0.406 *	M
2 13-10 3	12-10 2	251300.766(70)	0.078	M
2 13 12 1 +	12 12 0 +	251418.194(70)	-0.012	M
2 13 12 2 -	12 12 1 -	251418.194(70)	-0.012	M
2 13 3 11 +	12 3 10 +	251743.210(70)	-0.032	M
2 13 3 10 -	12 3 9 -	251939.163(70)	-0.065	M
2 13 7 6 -	12 7 5 -	252330.634(70)	0.069	M
2 13 7 7 +	12 7 6 +	252330.634(70)	0.069	M
2 13 -5 8	12 -5 7	253048.622(70)	0.045	M
2 13 8 6	12 8 5	253251.551(70)	0.028	M
2 13 4 9	12 4 8	253431.336(70)	-0.041	M
2 13 11 2 -	12 11 1 -	253623.016(70)	0.102	M
2 13 11 3 +	12 11 2 +	253623.016(70)	0.102	M
2 16 1 15	15 2 13	253695.093	-0.371 *	M
2 11 2 9 +	11 1 10 -	254194.298	0.186 *	M
2 13 10 3 +	12 10 2 +	254923.758(70)	-0.001	M
2 13 10 4 -	12 10 3 -	254923.758(70)	-0.001	M
2 8 3 6 +	9 2 7 +	255351.472(70)	0.113	M
2 13 2 11 +	12 2 10 +	255476.298(70)	0.000	M
2 13-11 2	12-11 1	255554.922(70)	0.051	M
2 13 9 4 -	12 9 3 -	255901.933(70)	0.293	M
2 13 9 5 +	12 9 4 +	255901.933(70)	0.132	M
2 13-12 1	12-12 0	256120.444	0.599 *	M
2 13 6 8	12 6 7	256307.495(70)	0.046	M
2 13 5 9	12 5 8	258094.466(70)	0.079	M
2 14 11 4	13 11 3	258104.646(70)	-0.136	M
2 10 2 8 +	10 1 9 -	258462.297(70)	-0.038	M
2 16 0 16 +	15 1 15 +	258531.589(70)	0.056	M
2 13 0 13	12 0 12	259762.028(70)	0.054	M
0 19 3 17 +	19 2 18 -	260283.520(70)	0.117	M
2 14 -8 6	13 -8 5	260911.342(70)	-0.099	M
2 19 -3 17	19 -2 18	260952.332	0.798 *	M
2 14 5 9 -	13 5 8 -	261957.353(70)	-0.108	M
2 14 5 10 +	13 5 9 +	261957.353(70)	-0.020	M
2 10 -1 10	9 -2 8	262110.420	-0.065 *	M
2 14 -1 14	13 -1 13	262370.384(70)	-0.004	M
2 14 1 14 +	13 1 13 +	262811.677(70)	0.045	M
2 10 1 10 +	9 0 9 +	263199.718(70)	0.067	M
2 14 3 11	13 3 10	263275.707(70)	0.051	M
2 4 -3 2	3 -2 2	264049.426	-0.513 *	M
2 14 2 12	13 2 11	264504.915(70)	0.028	M
2 14 6 8 +	13 6 7 +	264588.931(70)	0.007	M
2 14 6 9 -	13 6 8 -	264588.931(70)	0.014	M
2 14 -7 7	13 -7 6	266172.115(70)	-0.071	M
2 15 0 15	15 -1 15	266463.808(70)	-0.088	M
2 20 1 19 -	20 0 20 +	267635.102(70)	0.024	M
2 14 0 14 +	13 0 13 +	267701.775(70)	0.003	M
2 14 -3 12	13 -3 11	268776.080(70)	0.060	M
2 9 2 7	8 1 7	270474.696(70)	-0.024	M
2 14 -6 8	13 -6 7	270610.356(70)	-0.020	M
2 14 12 2 +	13 12 1 +	270744.219(70)	-0.110	M
2 14 12 3 -	13 12 2 -	270744.219(70)	-0.110	M
2 14 1 13	13 1 12	270832.784(70)	0.135	M
2 14 2 13 -	13 2 12 -	271008.332(70)	-0.004	M
2 17 1 16	16 2 14	271939.971(70)	0.000	M
2 14 -5 9	13 -5 8	272582.219(70)	-0.005	M
2 14 8 7	13 8 6	272763.899(70)	-0.094	M
2 6 2 4 +	6 1 5 -	274586.242(70)	0.221	M
2 14 -4 11	13 -4 10	274674.114(70)	0.016	M
2 14-11 3	13-11 2	275095.057(70)	-0.063	M
2 14 2 12 +	13 2 11 +	275561.758(70)	0.002	M
2 14 9 5 -	13 9 4 -	275606.117	0.375 *	M
2 14 9 6 +	13 9 5 +	275606.117	-0.487 *	M
2 14-12 2	13-12 1	275828.268(70)	-0.109	M
2 15 11 5	14 11 4	277118.090(70)	-0.150	M
2 11 1 11 +	10 0 10 +	277248.747(70)	0.058	M
2 14 5 10	13 5 9	277693.826(70)	0.043	M
2 5 2 3 +	5 1 4 -	277899.092(70)	0.197	M
2 14 0 14	13 0 13	278530.160(70)	-0.011	M
2 14 1 13 -	13 1 12 -	279098.021(70)	0.015	M
2 15 -1 15	14 -1 14	280752.528(70)	-0.066	M
2 15 5 10 -	14 5 9 -	281000.579(70)	-0.099	M
2 15 5 11 +	14 5 10 +	281000.579(70)	0.080	M
0 15 0 15 +	14 0 14 +	281126.994(70)	0.026	M
2 11 -1 11	10 -2 9	281276.019(70)	0.068	M
2 15 1 15 +	14 1 14 +	281420.168(70)	0.026	M
2 17 0 17 +	16 1 16 +	281451.373(70)	-0.096	M
2 15 3 12	14 3 11	282264.517(70)	-0.021	M
2 15 6 9 +	14 6 8 +	283509.560(70)	0.006	M
2 15 6 10 -	14 6 9 -	283509.560(70)	0.021	M
2 15 -2 14	14 -2 13	284238.341(70)	-0.024	M
2 15 10 6	14 10 5	284353.955	-0.323 *	M
2 18 -2 17	17 -1 17	284839.158(70)	-0.026	M
2 2 2 0 +	2 1 1 -	284948.132(70)	0.200	M
2 15 -7 8	14 -7 7	285236.709	-0.869 *	M
2 15 2 13	14 2 12	285447.814(70)	0.025	M
2 18 1 17	17 2 15	286059.198(70)	0.156	M
2 15 0 15 +	14 0 14 +	286190.919(70)	0.051	M
2 15 4 12 -	14 4 11 -	286416.263	0.259 *	M
2 15 4 11 +	14 4 10 +	286427.731	-0.296 *	M
2 21 1 20 -	21 0 21 +	287030.100(70)	0.018	M
0 16 0 16 +	15 1 15 +	288004.146	0.338 *	M
2 15 -3 13	14 -3 12	288004.146	-0.726 *	M
2 15 -6 9	14 -6 8	289970.324	0.300 *	M
2 15 2 14 -	14 2 13 -	290219.254	0.571 *	M
2 15 7 8 -	14 7 7 -	290234.114(70)	-0.111	M
2 15 7 9 +	14 7 8 +	290297.990(70)	-0.116	M
2 15 7 9 +	14 7 8 +	290297.990(70)	-0.119	M
2 15 3 13 +	14 3 12 +	290550.319(70)	-0.153	M
2 15 4 11	14 4 10	290845.886(70)	-0.097	M

[a]Upper and lower state quantum numbers are indicated by ' and ", respectively. Torsion-rotation levels of A species have a ± "parity" label. Those of E species have a signed K_a value. The quantum number v_t indicates the torsional state. J, K_a and K_c are the usual asymmetric rotor rotational quantum numbers. P is the parity.

[b]Measured frequencies in MHz. Lines with an * were excluded from the fit. Others have their experimental uncertainty in kHz in parentheses.

[c]Residuals from the present fit (Tables III-VII) are given in the O-C columns in MHz.

[d]The letters M, Q and V indicate, respectively, measurements from RAD-2 in Nizhny Novgorod, measurements from NIST, and measurements from Lille.

TABLE 4—*Continued*

v_t J' K_a' K_c' P' J" K_a" K_c" P"	Frequency	O-C Lit	v_t J' K_a' K_c' P' J" K_a" K_c" P"	Frequency	O-C Lit	v_t J' K_a' K_c' P' J" K_a" K_c" P"	Frequency	O-C Lit
2 12 1 12+ 11 0 11+	291105.579	0.483 * M	2 13 -1 13 12 -2 11	316359.298(70)	-0.081 V	0 18 10 9- 17 10 8-	346806.083	0.640 * M
2 4 1 3 3 0 3	291308.187	-0.663 * M	2 16 5 12 15 5 11	316597.956(70)	-0.012 V	2 18 9 10 17 9 9	347897.524(70)	0.183 M
2 15 -5 10 14 -5 9	292131.038	-0.675 * M	1 17 1 17 16 1 16	316649.248(70)	0.079 M	2 20 0 20+ 19 1 19+	348367.408(70)	-0.044 M
2 15 8 8 14 8 7	292283.201(70)	0.033 M	2 17 -1 17 16 -1 16	317590.107(70)	-0.054 M	1 19 0 19+ 18 1 18+	348592.536(70)	-0.141 M
2 15 11 4- 14 11 3-	292682.998(70)	0.117 M	2 17 -8 9 16 -8 8	317971.320(70)	0.038 M	2 18 3 16+ 17 3 15+	348749.176(70)	0.104 M
2 15 11 5+ 14 11 4+	292682.998(70)	0.117 M	2 16 1 15- 15 1 14-	318358.879(70)	0.013 M	2 18 3 15- 17 3 14-	349752.639(70)	0.138 M
2 11 2 9 10 1 9	292830.652(70)	0.177 M	2 10 2 9- 10 1 10+	318371.822(70)	0.113 V	2 18 0 18 17 0 17	350585.696(70)	-0.006 M
2 15 7 9 14 7 8	293937.566(70)	0.002 M	2 14 1 14+ 13 0 13+	318535.147(70)	0.104 M	2 18 2 16 17 2 15	350601.243(70)	0.048 M
2 15 10 5+ 14 10 4+	294204.155(70)	-0.013 M	2 17 1 17+ 16 1 16+	318554.655(70)	0.013 M	2 18 -5 13 17 -5 12	350889.272	-0.390 * M
2 15 10 6- 14 10 5-	294204.155(70)	-0.015 M	2 17 3 14 16 3 13	320574.131(70)	0.000 M	2 18 11 7- 17 11 6-	351313.919(70)	0.156 M
2 15 -4 12 14 -4 11	294587.852(70)	0.026 M	2 8 0 8 7 -1 7	320738.085	-0.802 * M	2 18 11 8+ 17 11 7+	351313.919(70)	0.156 M
2 7 0 7 6 -1 6	294757.914	-0.148 * M	2 17 6 11+ 16 6 10+	321402.624(70)	0.044 M	0 6 3 3- 5 2 4-	351589.000(70)	0.052 M
2 15-12 3 14-12 2	295552.567(70)	-0.197 M	2 17 6 12- 16 6 11-	321402.624(70)	0.103 M	2 13 3 10 12 2 10	352311.007(70)	-0.006 M
2 15 2 13+ 14 2 12+	295706.336(70)	-0.013 M	2 17 -2 16 16 -2 15	321843.210(70)	-0.042 M	2 18 7 12 17 7 11	353005.682(70)	0.044 M
2 15 6 10 14 6 9	295935.470(70)	0.176 M	2 17 0 17+ 16 0 16+	322921.196(70)	0.131 M	2 18 10 8+ 17 10 7+	353171.085(70)	-0.005 M
2 16 11 6 15 11 5	296210.901(70)	-0.107 M	0 16 4 12+ 16 3 13-	323537.908(70)	0.083 M	2 18 10 9- 17 10 8-	353171.085(70)	-0.077 M
2 19 1 18 18 2 16	296776.548(70)	-0.043 M	2 6 1 5 5 0 5	323596.636(70)	-0.045 M	0 19 0 19+ 18 0 18+	353426.295(70)	0.007 M
2 15 0 15 14 0 14	296958.976(70)	-0.019 M	2 11 2 10- 11 1 11+	324760.696(70)	0.164 M	2 19 11 9 18 11 8	353929.279(70)	0.262 M
2 15 5 11 14 5 10	297196.333(70)	0.068 M	2 17 4 14- 16 4 13-	324806.679(70)	0.111 M	1 18 2 16+ 17 2 15+	354457.680(70)	0.085 M
2 17 0 17 17 -1 17	297712.052(70)	-0.177 M	2 17 4 13+ 16 4 12+	324836.459(70)	-0.099 M	2 18-12 6 17-12 5	354887.055	-0.630 * M
2 6 3 3- 7 2 6-	298420.621(70)	-0.123 M	2 17 1 16 16 1 15	325277.842(70)	0.044 M	2 18 5 14 17 5 13	355106.083(70)	-0.099 M
2 15 1 14- 14 1 13-	298761.369(70)	0.003 M	2 19 0 19 19 -1 19	325931.688(70)	-0.149 M	2 18 6 13 17 6 12	355353.949(70)	0.031 M
2 16 -8 8 15 -8 7	298916.404(70)	-0.063 M	2 19 0 19+ 18 1 18+	326390.075(70)	-0.034 M	2 19 1 19+ 18 1 18+	355580.601(70)	-0.049 M
2 16 1 16+ 15 1 15+	300001.139(70)	0.010 M	2 17-10 7 16-10 6	326772.234(70)	0.051 M	2 19 -8 11 18 -8 10	356163.494(70)	0.028 M
2 16 5 11- 15 5 10-	300077.470	-0.234 * M	2 17 7 10- 16 7 9-	328121.711(70)	-0.087 M	2 15 2 14- 15 1 15+	356339.569(70)	-0.006 M
2 16 5 12+ 15 5 11+	300077.470	0.118 * M	2 17 7 11+ 16 7 10+	328121.711(70)	-0.101 M	2 18 2 16+ 17 2 15+	356376.182(70)	0.003 M
2 16 3 13 15 3 12	301351.010(70)	0.053 M	2 17 2 16- 16 2 15-	328544.910(70)	0.058 M	2 18 1 17- 17 1 16-	357326.299(70)	0.028 M
2 16 6 10+ 15 6 9+	302446.749(70)	-0.010 M	2 17 9 9 16 9 8	328561.580(70)	0.024 M	2 19 -2 18 18 -2 17	358965.607(70)	-0.030 M
2 16 6 11- 15 6 10-	302446.749(70)	0.020 M	2 17 2 15 16 2 14	328960.197(70)	-0.089 M	2 19 0 19+ 18 0 18+	359391.353(70)	0.007 M
2 7 2 6- 7 1 7+	302784.817(70)	0.160 M	2 17 3 15+ 16 3 14+	329354.788(70)	0.018 M	2 17 1 17+ 16 0 16+	360024.215(70)	-0.023 M
2 16 -2 15 15 -2 14	303101.303(70)	-0.079 M	2 17 3 14- 16 3 13-	330109.898(70)	-0.158 M	2 19 10 10 18 10 9	360379.584	-0.689 * M
2 18 0 18+ 17 1 17+	304079.765(70)	0.028 M	2 20 -2 19 19 -1 19	330674.506	-0.359 * M	2 4 2 3- 3 1 2-	360751.582(70)	0.253 M
2 16 -7 9 15 -7 8	304313.374(70)	-0.208 M	2 17 -5 12 16 -5 11	331283.918(70)	0.005 M	2 19 1 18 18 1 17	361318.679(70)	-0.065 M
2 16 0 16+ 15 0 15+	304594.120(70)	0.042 M	2 17 8 10 16 8 9	331342.644(70)	0.071 M	2 19 -7 12 18 -7 11	361608.909(70)	-0.063 M
2 13 1 13+ 12 0 12+	304842.652(70)	0.012 M	2 12 2 11- 12 1 12+	331751.165	0.272 * M	2 16 -1 16 15 -2 14	362978.839(70)	0.116 M
2 20 1 19 19 2 17	305419.093(70)	-0.009 M	2 17 11 6- 16 11 5-	331764.393(70)	0.133 M	2 19 4 16- 18 4 15-	363248.401(70)	0.020 M
2 16 2 14 15 2 13	307033.147	-0.143 * M	2 17 11 7+ 16 11 6+	331764.393(70)	0.133 M	2 19 4 15+ 18 4 14+	363316.059(70)	-0.022 M
2 16 -3 14 15 -3 13	307286.207(70)	0.004 M	2 12 3 9 11 2 9	332152.200(70)	-0.040 M	2 9 1 8 8 0 8	364272.458(70)	0.247 M
2 8 2 7- 8 1 8+	307387.890	0.451 * M	2 15 1 15+ 14 0 14+	332253.427(70)	0.014 M	2 19-10 9 18-10 8	364515.184(70)	-0.246 M
2 16 1 15 15 1 14	307573.054(70)	0.006 M	2 14 -1 14 13 -2 12	332560.179(70)	-0.085 M	2 19 2 18- 18 2 17-	366731.560(70)	0.012 M
2 16 7 9- 15 7 8-	309223.929(70)	-0.062 V	2 17 0 17 16 0 16	332927.141(70)	0.130 M	2 19 9 11 18 9 10	367235.239(70)	0.075 M
2 16 7 10+ 15 7 9+	309223.929(70)	-0.069 V	2 17 7 11 16 7 10	333304.508(70)	0.022 M	2 19 0 19 18 0 18	368121.318	-0.360 * M
2 16 9 8 15 9 7	309227.484(70)	0.025 V	2 17 8 9+ 16 8 8+	333419.705(70)	-0.310 M	2 19 3 17+ 18 3 16+	368133.664(70)	-0.090 M
2 16 12 4+ 15 12 3+	309377.634(70)	-0.231 M	2 17 8 10- 16 8 9-	333419.705(70)	-0.113 M	2 19 3 16- 18 3 15-	369444.259(70)	0.065 M
2 16 12 5- 15 12 4-	309377.634(70)	-0.231 M	2 17 10 7+ 16 10 6+	333508.537(70)	-0.014 M	2 21 0 21+ 20 1 20+	370006.755(70)	-0.017 M
2 16 4 12 15 4 11	309576.707(70)	-0.196 M	2 17 10 8- 16 10 7-	333508.537(70)	-0.035 M	2 19 8 12 18 8 11	370430.560(70)	0.163 M
2 16 3 14+ 15 3 13+	309954.258(70)	0.020 M	2 18 11 8 17 11 7	334623.891	0.277 * M	2 19 11 8- 18 11 7-	370869.520(70)	0.085 M
2 16 3 13- 15 3 12-	310512.204(70)	0.079 M	2 17 -4 14 16 -4 13	334666.479	0.294 * M	2 19 11 9+ 18 11 8+	370869.520(70)	0.085 M
1 8 4 5- 8 3 6+	311183.740(70)	0.601 M	2 17 6 12 16 6 11	335561.178(70)	0.184 M	2 19 2 17 18 2 16	371392.366(70)	-0.034 M
2 16 -5 11 15 -5 10	311698.389(70)	-0.060 M	2 17 5 13 16 5 12	335899.578(70)	-0.044 M	2 14 3 11 13 2 11	371439.443(70)	-0.231 M
2 16 8 9 15 8 8	311809.503	0.193 * M	2 18 -1 18 17 -1 17	336025.659(70)	-0.015 M	2 19 7 13 18 7 12	372716.733(70)	0.059 M
2 16 11 5- 15 11 4-	312220.857(70)	0.137 V	2 17 2 15+ 16 2 14+	336127.558(70)	0.024 M	2 19 10 9+ 18 10 8+	372841.816(70)	0.144 M
2 16 11 6+ 15 11 5+	312220.857(70)	0.137 V	2 18 1 18+ 17 1 17+	337080.978(70)	0.003 M	2 19 10 10- 18 10 9-	372841.816(70)	-0.086 M
2 9 2 8- 9 1 9+	312581.849(70)	0.035 M	2 17 1 16- 16 1 15-	337883.086(70)	-0.012 M	2 20 -1 20 19 -1 19	372893.807(70)	0.027 M
2 21 1 20 20 2 18	313586.988(70)	-0.134 V	1 5 -3 2 4 -2 2	338103.555	0.191 * M	2 20 11 10 19 11 9	373288.019(70)	0.194 M
2 16 10 6+ 15 10 5+	313853.077(70)	-0.055 M	2 7 -3 5 6 -2 5	339269.099	0.603 * M	2 20 1 20+ 19 1 19+	374054.382(70)	-0.013 M
2 16 10 7- 15 10 6-	313853.077(70)	-0.060 M	2 13 2 12- 13 1 13+	339344.367(70)	0.037 M	2 18 1 18+ 17 0 17+	374184.190(70)	0.042 M
2 16 8 8+ 15 8 7+	314076.141(70)	-0.197 M	2 18 3 15 17 3 14	340008.033(70)	0.035 M	2 19 5 15 18 5 14	374226.027(70)	-0.128 M
2 16 8 9- 15 8 8-	314076.141(70)	-0.206 M	2 18 6 12+ 17 6 11+	340378.759(70)	-0.040 M	2 19-12 7 18-12 6	374746.874	-0.872 * M
2 16-11 5 15-11 4	314226.672	-0.656 * V	2 18 6 13- 17 6 12-	340378.759(70)	0.070 M	2 19 6 14 18 6 13	375121.258(70)	0.017 M
2 16 -4 13 15 -4 12	314581.626(70)	0.098 M	2 18 -2 17 17 -2 16	340463.426(70)	-0.009 M	2 19 -4 16 18 -4 15	375142.291	0.480 * M
2 6 -3 4 5 -2 4	314636.413	0.016 * M	2 18 0 18+ 17 0 17+	341182.926(70)	0.015 M	0 20 1 20+ 19 0 19+	375603.630(70)	0.016 M
1 16 2 14+ 15 2 13+	314754.937(70)	0.002 V	2 18 10 9 17 10 8	341350.965	-0.603 * M	2 17 2 16- 17 1 17+	375726.813(70)	-0.051 M
2 16 0 16 15 0 15	315074.604	0.322 * M	2 18 -7 11 17 -7 10	342498.909(70)	-0.111 M	2 19 2 17+ 18 2 16+	376629.415(70)	0.010 M
2 16 9 7- 15 9 6-	315120.501(70)	-0.043 M	2 18 1 17 17 1 16	343079.317(70)	-0.039 M	2 19 1 18- 18 1 17-	376680.344(70)	0.016 M
2 16 9 8+ 15 9 7+	315142.092(70)	-0.513 V	2 3 2 2- 2 1 1-	343198.020	-0.224 * M	2 20 -2 19 19 -2 18	377358.415	0.598 * M
2 16-12 4 15-12 3	315298.808(70)	-0.319 M	2 15 2 13 14 1 13	343368.222(70)	0.000 M	2 17 -1 17 16 -2 15	377467.511(70)	0.008 M
2 17 11 7 16 11 6	315381.490(70)	-0.045 M	2 18 4 15- 17 4 14-	344021.620(70)	0.079 M	2 20 0 20+ 19 0 19+	377558.030(70)	0.037 M
2 16 6 11 15 6 10	315751.955(70)	0.024 M	2 18 4 14+ 17 4 13+	344066.683	-0.416 * M	2 5 2 4- 4 1 3-	377681.937(70)	0.038 M
2 16 2 14+ 15 2 13+	315899.309(70)	-0.005 M	2 18-10 8 17-10 7	345633.899(70)	-0.177 M	2 20 10 11 19 10 10	379372.462	-0.655 * M
2 13 2 11 12 1 11	315966.418(70)	0.065 M	0 18 10 8+ 17 10 7+	346806.083	0.641 * M	2 20 1 19 19 1 18	380034.865(70)	-0.046 M

all data in the present fit (including lines treated in Ref. (*5*) and not presented again here) is given in Table 7, where weighted (unitless) root-mean-square deviations are given for transitions grouped according to vibrational quantum number v_t and measurement accuracy. To facilitate comparison of Table 7 with its analog, Table IV in Ref. (*5*), most of the new measurements have been placed in their own measurement-uncertainty categories of 70 and 180 kHz. It can be seen that the number of lines and quality of fit for other uncertainty categories is similar here to that in Ref. (*5*). The larger unitless rms deviations for the 70 and 130–200 kHz categories (compared to those for neighboring categories) suggests that the present theoretical model is not capable of fitting transitions involving the $v_t = 3$ and 4 levels of acetaldehyde to microwave accuracy.

As might be expected, however, fitting difficulties are not evenly distributed among the torsion–*K*-rotation levels. The majority of the precision measurements in Table 5, which all involve torsional states below the barrier, are fit to 100 kHz or so. The situation is quite different, however, for the $v_t = 3$ and 4 transitions considered here, which lie above the barrier but below ν_{10}. Most of the $v_t = 3$ *A* levels with $0 \leqslant K \leqslant 9$, which according to Fig. 3 (see also Fig. 4 for v_t and *A*, *E* labels) do not have any perturbation partners

TABLE 5

Assignments,[a] Observed Values,[b] Residuals from the Fit,[c] and Sources[d] for Microwave Transitions within the v_t = 3 and 4 States

v_t	J'	K_a'	K_c'P'	J"	K_a"	K_c"P"	Frequency	O-C	Lit
3	1	0	1+	0	0	0+	19589.307(40)	-0.014	E
3	2	0	2+	1	0	1+	39180.854(40)	0.045	E
3	3	0	3+	2	0	2+	58776.650(70)	0.006	Q
3	7	0	7+	6	0	6+	137248.147(180)	0.110	T
3	8	0	8+	7	0	7+	156899.705(70)	0.231	V
3	9	0	9+	8	0	8+	176569.484(990)	0.247	X
3	10	0	10+	9	0	9+	196260.266(990)	0.307	X
3	11	0	11+	10	0	10+	215974.470(990)	0.040	X
3	12	0	12+	11	0	11+	235716.175(990)	0.525	X
3	14	0	14+	13	0	13+	275291.911(990)	0.057	X
3	15	0	15+	14	0	14+	295134.128	-0.587 *	X
3	16	0	16+	15	0	15+	315021.256	0.824 *	V
3	17	0	17+	16	0	16+	334955.808(990)	0.847	X
3	18	0	18+	17	0	17+	354946.722(990)	1.130	X
3	19	0	19+	18	0	18+	375002.343(990)	1.039	X
3	20	0	20+	19	0	19+	395134.411(990)	1.362	X
3	21	0	21+	20	0	20+	415355.742(990)	1.984	X
3	2	1	1-	1	1	0-	39745.954(40)	-0.031	E
3	3	1	2-	2	1	1-	59625.960(70)	-0.056	Q
3	6	1	5-	5	1	4-	119329.710(180)	0.057	T
3	7	1	6-	6	1	5-	139262.907(180)	0.079	T
3	8	1	7-	7	1	6-	159218.067(70)	0.014	V
3	9	1	8-	8	1	7-	179199.266(990)	-0.217	X
3	10	1	9-	9	1	8-	199211.845(990)	0.247	X
3	11	1	10-	10	1	9-	219259.025(990)	-0.017	X
3	12	1	11-	11	1	10-	239347.235	0.963 *	X
3	13	1	12-	12	1	11-	259476.324(990)	-0.613	X
3	14	1	13-	13	1	12-	279651.637(990)	-1.276	X
3	15	1	14-	14	1	13-	299873.108(70)	0.169	V
3	16	1	15-	15	1	14-	320131.637(990)	0.758	X
3	18	1	17-	17	1	16-	360700.110(990)	0.333	X
3	19	1	18-	18	1	17-	380958.449(990)	1.362	X
3	20	1	19-	19	1	18-	401144.167(990)	0.651	X
3	2	1	2+	1	1	1+	38962.253	0.477 *	T
3	3	1	3+	2	1	2+	58449.629(180)	0.056	T
3	6	1	6+	5	1	5+	116976.776(180)	-0.057	T
3	7	1	7+	6	1	6+	136518.786(180)	-0.226	T
3	8	1	8+	7	1	7+	156085.247(70)	0.355	V
3	9	1	9+	8	1	8+	175680.807(990)	0.982	X
3	12	1	12+	11	1	11+	234706.234(70)	0.706	V
3	16	1	16+	15	1	15+	314248.939	1.267 *	V
3	17	1	17+	16	1	16+	334311.810(990)	1.825	X
3	18	1	18+	17	1	17+	354427.893(990)	1.602	X
3	19	1	19+	18	1	18+	374571.249(990)	1.955	X
3	20	1	20+	19	1	19+	394700.445(990)	2.102	X
3	21	1	21+	20	1	20+	414763.828(990)	2.275	X
3	3	2	2-	2	2	1-	59871.900(70)	-0.052	Q
3	6	2	5-	5	2	4-	119642.931(180)	0.145	T
3	7	2	6-	6	2	5-	138984.345(180)	0.195	T
3	8	2	7-	7	2	6-	157880.242(70)	0.293	V
3	9	2	8-	8	2	7-	176465.420(990)	0.743	X
3	11	2	10-	10	2	9-	213460.476(990)	0.648	X
3	12	2	11-	11	2	10-	232058.519(70)	0.304	V
3	13	2	12-	12	2	11-	250739.482	-0.923 *	X
3	14	2	13-	13	2	12-	269494.246(990)	0.587	X
3	15	2	14-	14	2	13-	288306.732(990)	0.695	X
3	16	2	15-	15	2	14-	307169.641(70)	0.169	V
3	17	2	16-	16	2	15-	326079.166(990)	-0.176	X
3	18	2	17-	17	2	16-	345033.388(990)	0.008	X
3	19	2	18-	18	2	17-	364030.482(990)	-0.271	X
3	21	2	20-	20	2	19-	402156.406(990)	0.743	X
3	3	2	1+	2	2	0+	59865.460(70)	0.182	Q
3	6	2	4+	5	2	3+	119586.143(180)	0.145	T
3	7	2	5+	6	2	4+	138898.579(180)	0.197	T
3	8	2	6+	7	2	5+	157762.450(70)	-0.481	V
3	9	2	7+	8	2	6+	176314.521(990)	-0.556	X
3	10	2	8+	9	2	7+	194758.458(990)	-0.004	X
3	11	2	9+	10	2	8+	213229.382(990)	0.189	X
3	14	2	12+	13	2	11+	269075.975(990)	0.658	X
3	15	2	13+	14	2	12+	287809.093(990)	1.166	X
3	16	2	14+	15	2	13+	306584.469(70)	0.323	V
3	17	2	15+	16	2	14+	325401.352	1.169 *	X
3	18	2	16+	17	2	15+	344255.193(990)	0.509	X
3	19	2	17+	18	2	16+	363147.792(990)	-0.005	X
3	20	2	18+	19	2	17+	382080.306(990)	-0.203	X
3	7	3	4-	6	3	3-	140881.815(180)	-0.472	T
3	8	3	5-	7	3	4-	157762.450(70)	-0.304	V
3	9	3	6-	8	3	5-	174865.220	-1.633 *	X
3	10	3	7-	9	3	6-	192174.709(990)	-0.476	X
3	11	3	8-	10	3	7-	209687.976(990)	-0.318	X
3	12	3	9-	11	3	8-	227402.238(70)	-0.192	V
3	13	3	10-	12	3	9-	245304.373(990)	-0.596	X
3	14	3	11-	13	3	10-	263376.665(990)	0.106	X
3	16	3	13-	15	3	12-	299936.448(70)	-0.007	V
3	17	3	14-	16	3	13-	318380.641(70)	0.031	V
3	18	3	15-	17	3	14-	336908.033(990)	-0.152	X
3	19	3	16-	18	3	15-	355502.917(990)	0.024	X
3	20	3	17-	19	3	16-	374151.628(990)	0.531	X
3	21	3	18-	20	3	17-	392842.109(990)	0.378	X
3	6	3	4+	5	3	3+	124346.994(180)	-0.081	T
3	7	3	5+	6	3	4+	140878.425(180)	-0.232	T
3	8	3	6+	7	3	5+	157755.117(70)	-0.336	V
3	11	3	9+	10	3	8+	209655.962(990)	0.101	X
3	12	3	10+	11	3	9+	227355.931(70)	-0.107	V
3	13	3	11+	12	3	10+	245241.828(990)	0.160	X
3	14	3	12+	13	3	11+	263293.247(990)	-0.142	X
3	16	3	14+	15	3	13+	299804.700(70)	0.071	V
3	17	3	15+	16	3	14+	318220.823(990)	0.871	X
3	18	3	16+	17	3	15+	336716.023(990)	0.382	X
3	20	3	18+	19	3	17+	373886.626(990)	1.148	X

v_t	J'	K_a'	K_c'P'	J"	K_a"	K_c"P"	Frequency	O-C	Lit
3	21	3	19+	20	3	18+	392535.423(990)	0.499	X
3	7	4	4-	6	4	3-	120209.369(180)	-0.326	T
3	10	4	7-	9	4	6-	180156.287	0.633 *	X
3	14	4	11-	13	4	10-	258719.600(990)	-0.683	X
3	16	4	13-	15	4	12-	298670.917(70)	-0.230	V
3	17	4	14-	16	4	13-	318279.484(70)	-0.290	V
3	18	4	15-	17	4	14-	337859.985(990)	0.441	X
3	19	4	16-	18	4	15-	357394.876(990)	-0.239	X
3	20	4	17-	19	4	16-	376876.348	-2.519 *	X
3	21	4	18-	20	4	17-	396304.308(990)	-0.484	X
3	7	4	3+	6	4	2+	120209.369(180)	0.276	T
3	14	4	10+	13	4	9+	258709.515(990)	0.570	X
3	16	4	12+	15	4	11+	298648.137(990)	0.122	X
3	17	4	13+	16	4	12+	318249.112(70)	-0.324	V
3	18	4	14+	17	4	13+	337820.354(990)	0.266	X
3	20	4	16+	19	4	15+	376812.459	-1.687 *	X
3	21	4	17+	20	4	16+	396223.062(990)	-0.015	X
3	6	5	2+	5	5	1+	120726.166(990)	0.639	T
3	6	5	1-	5	5	0-	120726.166(990)	-1.085	T
3	7	5	3+	6	5	2+	141674.064(180)	-0.075	T
3	7	5	2-	6	5	1-	141681.373	-0.757 *	T
3	9	5	4-	8	5	3-	184513.857(990)	-0.070	X
3	9	5	5+	8	5	4+	184461.457(990)	1.060	X
3	10	5	5-	9	5	4-	205905.177(990)	-1.146	X
3	10	5	6+	9	5	5+	205809.699(990)	-0.179	X
3	11	5	6-	10	5	5-	227007.592(70)	-0.370	V
3	11	5	7+	10	5	6+	226854.124(70)	-0.363	V
3	12	5	7-	11	5	6-	247745.182(990)	-0.204	X
3	13	5	9+	12	5	8+	267782.105(990)	0.126	X
3	14	5	9-	13	5	8-	288105.220(990)	0.428	X
3	15	5	10-	14	5	9-	307739.694(70)	-0.167	V
3	15	5	11+	14	5	10+	307119.970(70)	-0.105	V
3	16	5	11-	15	5	10-	326983.911(990)	-0.202	X
3	16	5	12+	15	5	11+	326165.136(990)	0.367	X
3	17	5	13+	16	5	12+	344695.887(990)	1.062	X
3	17	5	12-	16	5	11-	345692.893(990)	0.516	X
3	18	5	14+	17	5	13+	362471.049(990)	0.521	X
3	18	5	13-	17	5	12-	363294.190(990)	0.150	X
3	19	5	15+	18	5	14+	379212.144(990)	0.125	X
3	20	5	15-	19	5	14-	400587.087	0.055 *	X
3	21	5	17+	20	5	16+	417373.048	-1.207 *	X
3	7	6	1+	6	6	0+	137150.027(180)	-0.042	T
3	7	6	2-	6	6	1-	137150.027(180)	-0.043	T
3	8	6	2+	7	6	1+	156780.826(70)	-0.171	V
3	8	6	3-	7	6	2-	156780.826(70)	-0.177	V
3	9	6	4-	8	6	3-	176428.394(990)	-0.309	X
3	9	6	3+	8	6	2+	176428.394(990)	-0.283	X
3	10	6	5-	9	6	4-	196096.253(990)	-0.055	X
3	10	6	4+	9	6	3+	196096.253(990)	0.043	X
3	11	6	6-	10	6	5-	215787.323(990)	-0.083	X
3	11	6	5+	10	6	4+	215787.323(990)	0.232	X
3	12	6	6+	11	6	5+	235505.235(70)	-0.022	V
3	13	6	8-	12	6	7-	255256.770(990)	-0.645	X
3	13	6	7+	12	6	6+	255256.770(990)	1.660	X
3	16	6	10+	15	6	9+	314744.420(70)	0.001	V
3	16	6	11-	15	6	10-	314769.795(70)	-0.046	V
3	17	6	12-	16	6	11-	334720.929(990)	-0.029	X
3	18	6	12+	17	6	11+	354651.665(990)	0.667	X
3	18	6	13-	17	6	12-	354745.125	-1.764 *	X
3	19	6	14-	18	6	13-	374860.718(990)	0.100	X
3	20	6	14+	19	6	13+	394772.037(990)	0.459	X
3	20	6	15-	19	6	14-	395076.657(990)	0.292	X
3	21	6	15+	20	6	14+	414896.340(990)	0.812	X
3	21	6	16-	20	6	15-	415408.592(990)	0.520	X
3	8	7	2+	7	7	1+	155967.282(70)	-0.242	V
3	8	7	1-	7	7	0-	155967.282(70)	-0.242	V
3	9	7	2-	8	7	1-	175473.791(990)	-0.181	X
3	9	7	3+	8	7	2+	175473.791(990)	-0.181	X
3	11	7	4-	10	7	3-	214499.333(990)	0.012	X
3	11	7	5+	10	7	4+	214499.333(990)	0.012	X
3	12	7	5-	11	7	4-	234019.633(990)	0.234	X
3	12	7	6+	11	7	5+	234019.633(990)	0.234	X
3	13	7	7+	12	7	6+	253545.104(990)	-0.153	X
3	13	7	6-	12	7	5-	253545.104(990)	-0.154	X
3	14	7	8+	13	7	7+	273077.575(990)	0.003	X
3	14	7	7-	13	7	6-	273077.575(990)	0.001	X
3	15	7	9+	14	7	8+	292617.493(990)	0.440	X
3	15	7	8-	14	7	7-	292617.493(990)	0.435	X
3	16	7	10+	15	7	9+	312164.389(70)	-0.055	V
3	16	7	9-	15	7	8-	312164.389(70)	-0.068	V
3	17	7	11+	16	7	10+	331720.895(990)	0.379	X
3	17	7	10-	16	7	9-	331720.895(990)	0.350	X
3	18	7	12+	17	7	11+	351286.251(990)	0.187	X
3	18	7	11-	17	7	10-	351286.251(990)	0.126	X
3	21	7	15+	20	7	14+	410048.316(990)	0.578	X
3	21	7	14-	20	7	13-	410048.316(990)	0.098	X
3	9	8	1+	8	8	0+	174935.090(990)	-0.048	X
3	9	8	2-	8	8	1-	174935.090(990)	-0.048	X
3	10	8	2+	9	8	1+	194369.366(990)	0.264	X
3	10	8	3-	9	8	2-	194369.366(990)	0.264	X
3	11	8	3+	10	8	2+	213801.838(990)	-0.080	X
3	11	8	4-	10	8	3-	213801.838(990)	-0.080	X
3	12	8	4+	11	8	3+	233233.447(70)	0.051	V
3	12	8	5-	11	8	4-	233233.447(70)	0.051	V
3	14	8	6+	13	8	5+	272091.397(990)	-0.007	X
3	14	8	7-	13	8	6-	272091.397(990)	-0.007	X
3	15	8	7+	14	8	6+	291516.769(990)	-0.574	X
3	15	8	8-	14	8	7-	291516.769(990)	-0.574	X
3	16	8	8+	15	8	7+	310940.781(70)	0.045	V
3	16	8	9-	15	8	8-	310940.781(70)	0.045	V

v_t	J'	K_a'	K_c'P'	J"	K_a"	K_c"P"	Frequency	O-C	Lit
3	17	8	9+	16	8	8+	330360.767(990)	-0.328	X
3	17	8	10-	16	8	9-	330360.767(990)	-0.328	X
3	18	8	10+	17	8	9+	349777.625(990)	-0.189	X
3	18	8	11-	17	8	10-	349777.625(990)	-0.189	X
3	19	8	11+	18	8	10+	369190.419(990)	0.282	X
3	19	8	12-	18	8	11-	369190.419(990)	0.282	X
3	20	8	12+	19	8	11+	388596.809(990)	-0.306	X
3	20	8	13-	19	8	12-	388596.809(990)	-0.308	X
3	1	0	1	0	0	0	19597.847(40)	0.036	E
3	2	0	2	1	0	1	39210.081(40)	0.030	E
3	3	0	3	2	0	2	58850.873(180)	0.133	T
3	6	0	6	5	0	5	118064.262(180)	0.071	T
3	7	0	7	6	0	6	137926.192(180)	0.134	T
3	8	0	8	7	0	7	157852.589(70)	0.137	V
3	9	0	9	8	0	8	177836.760(990)	0.746	X
3	10	0	10	9	0	9	197862.023	-1.057 *	X
3	11	0	11	10	0	10	217915.008(990)	0.237	X
3	12	0	12	11	0	11	237969.736(990)	0.610	X
3	13	0	13	12	0	12	258004.251(990)	0.441	X
3	14	0	14	13	0	13	277999.047(990)	0.328	X
3	15	0	15	14	0	14	297938.220(70)	0.323	V
3	16	0	16	15	0	15	317811.107(990)	0.599	X
3	17	0	17	16	0	16	337611.648(990)	0.716	X
3	20	0	20	19	0	19	396589.431(990)	1.221	X
3	21	0	21	20	0	20	416125.361(990)	0.877	X
3	2	1	2	1	1	1	38339.646(180)	-0.072	T
3	3	1	3	2	1	2	57529.742(70)	0.180	Q
3	7	1	7	6	1	6	134505.575(180)	-0.113	T
3	9	1	9	8	1	8	173094.031(990)	-0.415	X
3	10	1	10	9	1	9	192395.505	1.599 *	X
3	11	1	11	10	1	10	211687.337(990)	0.664	X
3	12	1	12	11	1	11	230965.017(990)	0.047	X
3	13	1	13	12	1	12	250221.523(990)	0.360	X
3	15	1	15	14	1	14	288639.124(990)	0.677	X
3	16	1	16	15	1	15	307784.953	-1.468 *	X
3	17	1	17	16	1	16	326886.822(990)	0.532	X
3	18	1	18	17	1	17	345934.150	0.866 *	X
3	19	1	19	18	1	18	364923.851(990)	0.299	X
3	20	1	20	19	1	19	383854.692(990)	0.426	X
3	21	1	21	20	1	20	402724.182(990)	0.449	X
3	2	-1	1	1	-1	0	39054.851(40)	-0.006	E
3	3	-1	2	2	-1	1	58585.636(70)	0.113	Q
3	6	-1	5	5	-1	4	117206.295(180)	-0.068	T
3	7	-1	6	6	-1	5	136760.995(180)	0.078	T
3	8	-1	7	7	-1	6	156325.368(70)	0.211	V
3	9	-1	8	8	-1	7	175901.625(990)	0.791	X
3	10	-1	9	9	-1	8	195490.026(990)	0.094	X
3	11	-1	10	10	-1	9	215096.296	1.552 *	X
3	12	-1	11	11	-1	10	234718.167(70)	0.210	V
3	13	-1	12	12	-1	11	254364.091	1.345 *	X
3	14	-1	13	13	-1	12	274032.739(990)	-0.126	X
3	16	-1	15	15	-1	14	313468.262(990)	0.852	X
3	17	-1	16	16	-1	15	333243.644(990)	0.937	X
3	18	-1	17	17	-1	16	353066.256	1.326 *	X
3	19	-1	18	18	-1	17	372941.286(990)	0.611	X
3	20	-1	19	19	-1	18	392877.791(990)	1.405	X
3	21	-1	20	20	-1	19	412878.505(990)	1.068	X
3	3	2	2	2	2	1	59090.870(70)	0.030	Q
3	6	2	5	5	2	4	117428.786(180)	-0.016	T
3	7	2	6	6	2	5	136621.138(180)	-0.048	T
3	9	2	8	8	2	7	174602.036	1.045 *	X
3	12	2	11	11	2	10	230737.893(990)	0.223	X
3	14	2	13	13	2	12	267845.863(990)	0.817	X
3	15	2	14	14	2	13	286364.220(990)	-0.398	X
3	16	2	15	15	2	14	304880.300(990)	-0.258	X
3	17	2	16	16	2	15	323401.463	-0.399 *	M
3	18	2	17	17	2	16	341933.907(990)	-0.017	X
3	19	2	18	18	2	17	360480.297(990)	0.835	X
3	20	2	19	19	2	18	379040.550(990)	1.074	X
3	21	2	20	20	2	19	397614.511(990)	0.367	X
3	22	2	21	21	2	20	416204.836(990)	1.208	X
3	3	-2	1	2	-2	0	58458.847(70)	0.070	Q
3	6	-2	4	5	-2	3	116929.458(180)	-0.207	T
3	7	-2	5	6	-2	4	136424.243(180)	-0.208	T
3	9	-2	7	8	-2	6	175422.528(990)	0.648	X
3	11	-2	9	10	-2	8	214427.045(990)	1.072	X
3	12	-2	10	11	-2	9	233922.257(990)	0.962	X
3	13	-2	11	12	-2	10	253377.565(990)	0.053	X
3	16	-2	14	15	-2	13	311809.503	-0.652 *	M
3	17	-2	15	16	-2	14	331497.675	2.266 *	X
3	18	-2	16	17	-2	15	351034.325(990)	0.705	X
3	21	-2	19	20	-2	18	409273.999(990)	1.867	X
3	6	3	4	5	3	3	117158.564(180)	-0.215	T
3	7	3	5	6	3	4	136716.945(180)	-0.044	T
3	8	3	6	7	3	5	156289.937(70)	0.010	V
3	9	3	7	8	3	6	175880.259(990)	0.772	X
3	11	3	9	10	3	8	215115.580	1.420 *	V
3	12	3	10	11	3	9	234760.890(990)	0.340	X
3	14	3	12	13	3	11	274107.196(990)	0.128	X
3	16	3	14	15	3	13	313502.386(990)	0.612	X
3	17	3	15	16	3	14	333200.126	-0.796 *	X
3	18	3	16	17	3	15	352887.902(990)	-0.165	X
3	19	3	17	18	3	16	372550.838(990)	0.284	X
3	20	3	18	19	3	17	392174.876(990)	0.868	X
3	21	3	19	20	3	18	411743.920(990)	0.755	X
3	6	-3	3	5	-3	2	123323.327	1.282 *	T
3	7	-3	4	6	-3	3	144219.615	1.326 *	T
3	8	-3	5	7	-3	4	165346.000(990)	0.900	X
3	9	-3	6	8	-3	5	186762.690	0.648 *	X
3	10	-3	7	9	-3	6	208452.888(990)	0.368	X

[a]Upper and lower state quantum numbers are indicated by ' and ", respectively. Torsion-rotation levels of A species have a ± "parity" label. Those of E species have a signed K_a value. The quantum number v_t indicates the torsional state. J, K_a and K_c are the usual asymmetric rotor rotational quantum numbers. P is the parity.

[b]Measured frequencies in MHz. Lines with an * were excluded from the fit. Others have their experimental uncertainty in kHz in parentheses, except that the entry (990) actually corresponds to an assigned uncertainty of 1000 kHz in the fit.

[c]Residuals from the present fit (Tables III-VII) are given in the O-C columns in MHz.

[d]Measurement sources are: E - Ref. (13); Q and T - NIST; V - Lille; and X - RAD-3 in Nizhny Novgorod.

TABLE 5—*Continued*

v_t	J'	K_a'	K_c'P'	J"	K_a"	K_c"P"	Frequency	O-C	Lit
3	11	-3	8	10	-3	7	230247.272	2.985	* X
3	12	-3	9	11	-3	8	251802.240	2.529	* X
3	14	-3	11	13	-3	10	292830.652(70)	0.014	M
3	15	-3	12	14	-3	11	312029.009(990)	-1.652	X
3	16	-3	13	15	-3	12	330462.575(990)	-2.293	X
3	17	-3	14	16	-3	13	348329.624	-3.166	* X
3	6	4	3	5	4	2	116876.356(180)	-0.038	T
3	7	4	4	6	4	3	136363.118(180)	-0.096	T
3	9	4	6	8	4	5	175347.849(990)	0.064	X
3	11	4	8	10	4	7	214350.053	-0.489	* X
3	12	4	9	11	4	8	233860.107(70)	-0.059	V
3	13	4	10	12	4	9	253377.565(990)	1.469	X
3	14	4	11	13	4	10	272900.105(990)	1.139	X
3	15	4	12	14	4	11	292427.980	-1.459	* X
3	17	4	14	16	4	13	331517.591(990)	1.724	X
3	18	4	15	17	4	14	351072.309(990)	-0.793	X
3	19	4	16	18	4	15	370640.389(990)	0.117	X
3	20	4	17	19	4	16	390218.127(990)	-0.211	X
3	10	-4	6	9	-4	5	216136.366(990)	0.540	X
3	11	-4	7	10	-4	6	232945.285	-0.638	* X
3	15	-4	11	14	-4	10	298208.846	-1.054	* X
3	16	-4	12	15	-4	11	315450.111(990)	-0.361	X
3	17	-4	13	16	-4	12	333038.658(990)	-0.194	X
3	18	-4	14	17	-4	13	350887.692(990)	-0.578	X
3	19	-4	15	18	-4	14	368928.563(990)	0.835	X
3	20	-4	16	19	-4	15	387105.669(990)	1.091	X
3	6	5	1	5	5	0	116635.144(180)	0.050	T
3	10	5	5	9	5	4	194402.533(990)	-0.021	X
3	11	5	6	10	5	5	213844.470	-2.154	* X
3	12	5	7	11	5	6	233291.534(990)	-0.208	X
3	13	5	8	12	5	7	252737.852(990)	-0.123	X
3	14	5	9	13	5	8	272186.973(990)	1.598	X
3	15	5	10	14	5	9	291632.880	-1.092	* X
3	16	5	11	15	5	10	311083.934(990)	0.184	X
3	17	5	12	16	5	11	330534.158(990)	-0.432	X
3	18	5	13	17	5	12	349984.717	-1.239	* X
3	20	5	15	19	5	14	388930.660(990)	-0.331	X
3	21	5	16	20	5	15	408336.083(990)	0.063	X
3	10	-5	6	9	-5	5	177437.700(990)	-0.720	X
3	11	-5	7	10	-5	6	195423.848(990)	-0.758	X
3	12	-5	8	11	-5	7	213844.470	1.910	* X
3	13	-5	9	12	-5	8	232513.794(70)	-0.078	V
3	11	6	5	10	6	4	170002.779	0.917	* X
3	12	6	6	11	6	5	190416.762(990)	0.150	X
3	13	6	7	12	6	6	211058.889(990)	0.361	X
3	14	6	8	13	6	7	231708.032(990)	-0.674	X
3	11	-6	6	10	-6	5	183994.058(990)	-0.019	X
3	12	-6	7	11	-6	6	204776.265(990)	-0.840	X
3	13	-6	8	12	-6	7	225451.401(990)	-0.415	X
3	10	7	3	9	7	2	167094.814(990)	0.618	X
3	11	7	4	10	7	3	189385.156(990)	-2.853	X
3	14	7	7	13	7	6	246421.315(990)	-2.714	X
3	15	7	8	14	7	7	264816.845(990)	-2.165	X
3	17	7	10	16	7	9	301786.635(990)	-0.825	X
3	15	7	8	14	7	7	264816.845(990)	-2.165	X
3	17	7	10	16	7	9	301786.635(990)	-0.825	X
3	18	7	11	17	7	10	320403.425(990)	-0.358	X
3	19	7	12	18	7	11	339102.481(990)	-0.477	X
3	20	7	13	19	7	12	357874.284(990)	1.740	X
3	21	7	14	20	7	13	376696.779	-2.541	* X

v_t	J'	K_a'	K_c'P'	J"	K_a"	K_c"P"	Frequency	O-C	Lit
3	22	7	15	21	7	14	395570.638(990)	-0.533	X
3	23	7	16	22	7	15	414477.962(990)	0.181	X
3	11	-7	5	10	-7	4	208335.308(990)	-2.551	X
3	12	-7	6	11	-7	5	226080.142(990)	-1.273	X
3	14	-7	8	13	-7	7	262391.364(990)	-0.884	X
3	15	-7	9	14	-7	8	280786.773(990)	-0.425	X
3	17	-7	11	16	-7	10	317885.794(990)	0.877	X
3	18	-7	12	17	-7	11	336554.962(990)	0.692	X
3	19	-7	13	18	-7	12	355289.878(990)	0.340	X
3	20	-7	14	19	-7	13	374085.377(990)	2.136	X
3	21	-7	15	20	-7	14	392931.544(990)	1.889	X
3	9	8	1	8	8	0	166326.931	0.194	* X
3	11	8	3	10	8	2	200299.510(990)	4.599	X
3	12	8	4	11	8	3	220049.963(990)	4.677	X
3	13	8	5	12	8	4	239950.771(990)	5.262	X
3	14	8	6	13	8	5	259691.587(990)	1.437	X
3	15	8	7	14	8	6	279136.316(990)	3.327	X
3	16	8	8	15	8	7	298208.846	4.856	* X
3	17	8	9	16	8	8	316885.634(990)	2.253	X
3	19	8	11	18	8	10	353215.038(990)	-0.603	X
3	9	-8	2	8	-8	1	182313.766(990)	-2.673	X
3	10	-8	3	9	-8	2	202998.592(990)	-1.866	X
3	11	-8	4	10	-8	3	223780.293(990)	-1.538	X
3	12	-8	5	11	-8	4	244613.575(990)	-1.037	X
3	12	-9	4	11	-9	3	236544.123(990)	-0.666	X
3	13	-9	5	12	-9	4	256384.206(990)	-0.421	X
3	14	-9	6	13	-9	5	276240.167(990)	-0.860	X
3	15	-9	7	14	-9	6	296107.943(990)	-2.386	X
3	17	-9	9	16	-9	8	335868.569(990)	-0.004	X
3	18	-9	10	17	-9	9	355745.477(990)	-0.313	X
3	19	-9	11	18	-9	10	375613.112(990)	0.584	X
3	20	-9	12	19	-9	11	395461.352(990)	0.432	X
3	21	-9	13	20	-9	12	415283.406(990)	0.991	X
4	1	0	1+	0	0	0+	19577.050(40)	-0.015	E
4	2	0	2+	1	0	1+	39153.803(40)	-0.113	E
4	3	0	3+	2	0	2+	58730.240(180)	-0.101	T
4	7	0	7+	6	0	6+	137027.152(180)	-0.612	T
4	8	0	8+	7	0	7+	156598.650(70)	-0.490	V
4	9	0	9+	8	0	8+	176168.114(990)	-0.908	X
4	12	0	12+	11	0	11+	234868.214(990)	-0.633	X
4	14	0	14+	13	0	13+	273992.857(990)	-1.035	X
4	15	0	15+	14	0	14+	293553.676(990)	-0.667	X
4	16	0	16+	15	0	15+	313113.485(990)	-0.335	X
4	17	0	17+	16	0	16+	332671.287(990)	-1.523	X
4	19	0	19+	18	0	18+	371790.784(990)	-1.445	X
4	20	0	20+	19	0	19+	391352.871(990)	-1.849	X
4	2	1	1-	1	1	0-	39465.339(180)	0.026	T
4	3	1	2-	2	1	1-	59198.755(180)	0.185	T
4	7	1	6-	6	1	5-	138141.150(180)	0.213	T
4	9	1	8-	8	1	7-	177620.197(990)	-0.367	X
4	10	1	9-	9	1	8-	197363.726(990)	0.637	X
4	11	1	10-	10	1	9-	217107.828(990)	0.230	X
4	12	1	11-	11	1	10-	236854.335(70)	0.137	V
4	13	1	12-	12	1	11-	256603.549(990)	0.577	X
4	14	1	13-	13	1	12-	276354.192(990)	0.213	X
4	15	1	14-	14	1	13-	296107.943(990)	0.687	X
4	16	1	15-	15	1	14-	315862.934(70)	0.114	V
4	17	1	16-	16	1	15-	335620.983(990)	0.317	X
4	20	1	19-	19	1	18-	394907.688(990)	0.056	X
4	2	1	2+	1	1	1+	38680.863(180)	-0.175	T

v_t	J'	K_a'	K_c'P'	J"	K_a"	K_c"P"	Frequency	O-C	Lit
4	3	1	3+	2	1	2+	58021.197(180)	-0.763	T
4	6	1	6+	5	1	5+	116046.533	-1.942	* T
4	12	1	12+	11	1	11+	232136.946	-3.270	* V
4	15	1	15+	14	1	14+	290228.510	3.159	* X
4	18	1	18+	17	1	17+	348353.937	-4.356	* X
4	19	1	19+	18	1	18+	367745.546	-5.229	* X
4	20	1	20+	19	1	19+	387148.353	-4.259	* X
4	21	1	21+	20	1	20+	406559.026	-6.187	* X
4	3	2	2-	2	2	1-	58521.013	-2.052	* T
4	6	2	5-	5	2	4-	117036.962	-5.188	* T
4	11	2	10-	10	2	9-	214545.208	-9.274	* X
4	12	2	11-	11	2	10-	234042.217	-10.554	* X
4	14	2	13-	13	2	12-	273032.234	-11.895	* X
4	15	2	14-	14	2	13-	292523.221	-13.743	* X
4	16	2	15-	15	2	14-	312013.718	-14.043	* X
4	18	2	17-	17	2	16-	350986.341	-16.539	* X
4	19	2	18-	18	2	17-	370469.575	-17.482	* X
4	3	2	1+	2	2	0+	58523.283	-2.749	* T
4	6	2	4+	5	2	3+	117062.517	-5.613	* T
4	7	2	5+	6	2	4+	136581.985	-6.545	* T
4	8	2	6+	7	2	5+	156105.736	-7.386	* V
4	9	2	7+	8	2	6+	175635.082	-7.433	* X
4	11	2	9+	10	2	8+	214707.328	-10.835	* X
4	13	2	11+	12	2	10+	253807.701	-12.718	* X
4	14	2	12+	13	2	11+	273368.319	-14.760	* X
4	16	2	14+	15	2	13+	312516.005	-18.574	* X
4	17	2	15+	16	2	14+	332103.348	-21.311	* X
4	18	2	16+	17	2	15+	351704.389	-20.723	* X
4	19	2	17+	18	2	16+	371309.728	-26.814	* X
4	21	2	19+	20	2	18+	410560.758	-33.941	* X
4	3	1	2	2	1	1	58613.153	0.172	* T
4	6	1	5	5	1	4	117232.271	0.511	* T
4	7	1	6	6	1	5	136774.571	0.907	* T
4	8	1	7	7	1	6	156318.769	1.667	* V
4	3	-1	3	2	-1	2	58933.546(180)	-0.079	T
4	6	-1	6	5	-1	5	117895.482(180)	-0.752	T
4	7	-1	7	6	-1	6	137561.095	-1.276	* T
4	8	-1	8	7	-1	7	157235.085	-1.595	* V
4	9	-1	9	8	-1	8	176918.902(990)	-1.719	X
4	3	-2	2	2	-2	1	59421.485(180)	0.393	T
4	6	-2	5	5	-2	4	118798.373(180)	0.346	T
4	7	-2	6	6	-2	5	138575.131(180)	0.445	T
4	9	-2	8	8	-2	7	178101.238(990)	-0.006	X
4	11	-2	10	10	-2	9	217595.128(990)	-0.124	X
4	12	-2	11	11	-2	10	237333.358(990)	-0.649	X
4	13	-2	12	12	-2	11	257070.923(990)	-0.484	X
4	14	-2	13	13	-2	12	276810.917(990)	-1.404	X
4	15	-2	14	14	-2	13	296561.647	-1.849	* V
4	16	-2	15	15	-2	14	316331.898	-2.168	* V
4	18	-2	17	17	-2	16	355982.150(990)	-3.416	X
4	21	-2	20	20	-2	19	416037.813	-2.041	* X
4	9	-3	7	8	-3	6	174416.146(990)	-3.116	X
4	11	-3	9	10	-3	8	213486.006(990)	-2.908	X
4	12	-3	10	11	-3	9	233178.181(990)	-1.948	X
4	9	-4	6	8	-4	5	175544.622(990)	-0.822	X
4	11	-4	8	10	-4	7	214606.758	-3.614	* X
4	12	-4	9	11	-4	8	234146.197	-5.366	* X
4	13	-4	10	12	-4	9	253696.164	-1.850	* X
4	14	-4	11	13	-4	10	273248.217	-0.802	* X
4	15	-4	12	14	-4	11	292799.403	-4.226	* X

nearby, are fit to 1 MHz or better in Table 4. On the other hand, the $K = 2$ $A\pm$ levels of $v_t = 4$, which lie just below ν_{10} in Fig. 3, seem to be pushed below their calculated values by 10 to 20 MHz. Even the $K = 1$ $A+$ levels of $v_t = 4$ seem to be pushed down by about 5 MHz. Most $v_t = 4$ E levels (which lie just below ν_{10}) also fit poorly. Attempts to reduce the residuals of the various problem transitions above by adding more terms to the torsion–rotation Hamiltonian all failed, so these transitions were ultimately excluded from the final fit. At this time we do not know which model deficiencies are responsible for these difficulties, but various not yet considered interactions with ν_{10} seem to be the most likely candidates.

Both the V_9 and V_{12} contributions to the barrier were determined in our final global fit. Even though V_{12} is of higher order than V_9, it is better determined in the fit, because the A_2 torsional level of $v_t = 3$ and the A_1 torsional level of $v_t = 4$ form a nearly degenerate $|m| = 6$ pair in the free-rotor limit, which is then split in first order by the cos 12γ term in the potential. The centrifugal distortion $J(J + 1)$ dependence of V_{12} is also well determined in the final fit, since this term (from another point of view) allows for different B values in the pair of split $|m| = 6$ states. Comparison of the present $v_t \leqslant 4$ fit with the $v_t \leqslant 2$ fit of Ref. (*5*) (see Table 3) shows that one fourth order term, nine sixth order terms, one eighth order term, and one tenth order term were added to the Hamiltonian, and that three sixth order terms were removed.

4. TORSION–ROTATION INTERACTIONS

A. Small Avoided Crossings near a Given J

Local perturbations affecting a half dozen J values and caused by avoided crossings with higher v_t levels were found in the calculated $v_t = 2$, $K = 9$, A and E levels of our previous study (*5*), but the levels involved were too poorly predicted to permit credible assignments in the perturbed regions. Hav-

TABLE 6

Assignments,[a] Observed Values,[b] and Residuals from the Fit[c] for Newly Assigned $\upsilon_t = 3 \leftarrow 2$ Far-Infrared Transitions

v_t'	J'	K_a'	$K_c'P'$	v_t''	J''	K_a''	$K_c''P''$	Waveno.	O-C	
3	6	6	1-	2	5	5	1+	92.7724	-0.0002	
3	6	6	0+	2	5	5	0-	92.7724	-0.0002	
3	7	6	2-	2	6	5	2+	93.6377	-0.0002	
3	7	6	1+	2	6	5	1-	93.6377	-0.0002	
3	8	6	3-	2	7	5	3+	94.5350	-0.0002	
3	8	6	2+	2	7	5	2-	94.5350	-0.0002	
3	9	6	4-	2	8	5	4+	95.4633	-0.0002	
3	9	6	3+	2	8	5	3-	95.4633	-0.0002	
3	10	6	5-	2	9	5	5+	96.4217	0.0000	
3	10	6	4+	2	9	5	4-	96.4217	0.0000	
3	11	6	6-	2	10	5	6+	97.4086	-0.0003	
3	11	6	5+	2	10	5	5-	97.4086	-0.0002	
3	12	6	7-	2	11	5	7+	98.4242	0.0000	
3	12	6	6+	2	11	5	6-	98.4242	0.0000	
3	13	6	8-	2	12	5	8+	99.4670	-0.0003	
3	13	6	7+	2	12	5	7-	99.4670	-0.0002	
3	14	6	9-	2	13	5	9+	100.5377	-0.0002	
3	14	6	8+	2	13	5	8-	100.5377	0.0001	
3	15	6	10-	2	14	5	10+	101.6356	-0.0005	
3	15	6	9+	2	14	5	9-	101.6356	0.0002	
3	16	6	11-	2	15	5	11+	102.7613	-0.0012	*
3	16	6	10+	2	15	5	10-	102.7613	0.0003	*
3	17	6	11+	2	16	5	11-	103.9149	0.0000	*
3	18	6	13-	2	17	5	13+	105.1039	-0.0005	
3	18	6	12+	2	17	5	12-	105.0973	-0.0006	
3	19	6	14-	2	18	5	14+	106.3227	-0.0006	
3	19	6	13+	2	18	5	13-	106.3106	-0.0003	
3	20	6	15-	2	19	5	15+	107.5769	-0.0006	
3	20	6	14+	2	19	5	14-	107.5554	0.0005	
3	6	6	1-	2	6	5	1-	89.0627	-0.0003	
3	6	6	0+	2	6	5	2+	89.0627	-0.0003	
3	7	6	2-	2	7	5	2-	89.3054	-0.0002	
3	7	6	1+	2	7	5	3+	89.3054	-0.0002	
3	8	6	3-	2	8	5	3-	89.5783	-0.0002	
3	8	6	2+	2	8	5	4+	89.5783	-0.0002	
3	9	6	4-	2	9	5	4-	89.8807	0.0001	
3	9	6	3+	2	9	5	5+	89.8807	0.0001	
3	10	6	5-	2	10	5	5-	90.2108	-0.0002	
3	10	6	4+	2	10	5	6+	90.2108	-0.0002	
3	11	6	6-	2	11	5	6-	90.5686	0.0000	
3	11	6	5+	2	11	5	7+	90.5686	0.0000	
3	12	6	7-	2	12	5	7-	90.9523	-0.0005	
3	12	6	6+	2	12	5	8+	90.9523	-0.0005	
3	13	6	8-	2	13	5	8-	91.3631	-0.0002	
3	13	6	7+	2	13	5	9+	91.3631	-0.0001	
3	14	6	9-	2	14	5	9-	91.7996	-0.0003	
3	14	6	8+	2	14	5	10+	91.7996	0.0000	
3	15	6	10-	2	15	5	10-	92.2625	-0.0004	
3	15	6	9+	2	15	5	11+	92.2625	0.0003	
3	16	6	11-	2	16	5	11-	92.7523	-0.0007	
3	16	6	10+	2	16	5	12+	92.7523	0.0008	
3	17	6	12-	2	17	5	12-	93.2689	-0.0023	*
3	17	6	11+	2	17	5	13+	93.2689	0.0009	*
3	18	6	13-	2	18	5	13-	93.8186	-0.0006	*
3	19	6	14-	2	19	5	14-	94.3988	-0.0002	
3	19	6	13+	2	19	5	15+	94.3868	-0.0001	
3	20	6	15-	2	20	5	15-	95.0131	-0.0002	
3	20	6	14+	2	20	5	16+	94.9903	-0.0008	
3	7	7	0-	2	6	6	0+	118.8904	-0.0007	
3	7	7	1+	2	6	6	1-	118.8904	-0.0007	
3	8	7	1-	2	7	6	1+	119.6772	-0.0006	
3	8	7	2+	2	7	6	2-	119.6772	-0.0006	
3	9	7	2-	2	8	6	2+	120.4843	-0.0011	
3	9	7	3+	2	8	6	3-	120.4843	-0.0011	
3	10	7	3-	2	9	6	3+	121.3141	0.0001	
3	10	7	4+	2	9	6	4-	121.3141	0.0001	
3	11	7	4-	2	10	6	4+	122.1636	-0.0002	
3	11	7	5+	2	10	6	5-	122.1636	-0.0002	
3	12	7	5-	2	11	6	5+	123.0345	-0.0005	
3	12	7	6+	2	11	6	6-	123.0345	-0.0005	
3	13	7	6-	2	12	6	6+	123.9278	0.0002	
3	13	7	7+	2	12	6	7-	123.9278	0.0002	
3	14	7	7-	2	13	6	7+	124.8405	-0.0009	
3	14	7	8+	2	13	6	8-	124.8405	-0.0009	
3	15	7	8-	2	14	6	8+	125.7761	-0.0002	
3	15	7	9+	2	14	6	9-	125.7761	-0.0002	
3	16	7	9-	2	15	6	9+	126.7320	-0.0001	
3	16	7	10+	2	15	6	10-	126.7320	-0.0001	
3	17	7	10-	2	16	6	10+	127.7079	-0.0007	
3	17	7	11+	2	16	6	11-	127.7079	-0.0007	
3	18	7	11-	2	17	6	11+	128.7041	-0.0013	
3	18	7	12+	2	17	6	12-	128.7041	-0.0013	
3	19	7	12-	2	18	6	12+	129.7195	-0.0027	*
3	19	7	13+	2	18	6	13-	129.7195	-0.0027	*
3	20	7	13-	2	19	6	13+	130.7584	-0.0002	
3	20	7	14+	2	19	6	14-	130.7584	-0.0002	
3	7	7	0-	2	7	6	2-	114.4755	0.0002	
3	7	7	1+	2	7	6	1+	114.4755	0.0002	
3	8	7	1-	2	8	6	3-	114.6295	-0.0027	*
3	8	7	2+	2	8	6	2+	114.6295	-0.0027	*
3	10	7	3-	2	10	6	5-	115.0087	-0.0002	
3	10	7	4+	2	10	6	4+	115.0087	-0.0002	
3	11	7	4-	2	11	6	6-	115.2290	0.0000	
3	11	7	5+	2	11	6	5+	115.2290	0.0000	
3	12	7	5-	2	12	6	7-	115.4702	0.0000	
3	12	7	6+	2	12	6	6+	115.4702	0.0000	
3	13	7	6-	2	13	6	8-	115.7307	-0.0018	*
3	13	7	7+	2	13	6	7+	115.7307	-0.0018	*
3	14	7	7-	2	14	6	9-	116.0150	-0.0006	
3	14	7	8+	2	14	6	8+	116.0150	-0.0006	
3	15	7	8-	2	15	6	10-	116.3189	-0.0005	
3	15	7	9+	2	15	6	9+	116.3189	-0.0005	
3	16	7	9-	2	16	6	11-	116.6430	-0.0006	
3	16	7	10+	2	16	6	10+	116.6430	-0.0006	
3	18	7	11-	2	18	6	13-	117.3516	0.0000	
3	18	7	12+	2	18	6	12+	117.3516	0.0000	
3	19	7	12-	2	19	6	14-	117.7345	-0.0002	
3	19	7	13+	2	19	6	13+	117.7345	-0.0002	
3	20	7	13-	2	20	6	15-	118.1378	0.0012	
3	20	7	14+	2	20	6	14+	118.1378	0.0012	
3	6	5	1-	2	5	4	1+	80.2885	0.0002	
3	6	5	2+	2	5	4	2-	80.2885	0.0003	
3	7	5	2-	2	6	4	2+	81.2008	-0.0001	
3	7	5	3+	2	6	4	3-	81.2008	0.0002	
3	8	5	3-	2	7	4	3+	82.1884	-0.0005	
3	8	5	4+	2	7	4	4-	82.1884	0.0006	
3	9	5	4-	2	8	4	4+	83.2565	-0.0009	*
3	9	5	5+	2	8	4	5-	83.2565	0.0020	*
3	10	5	5-	2	9	4	5+	84.4029	0.0003	
3	10	5	6+	2	9	4	6-	84.3968	0.0004	
3	11	5	6-	2	10	4	6+	85.6137	-0.0005	
3	11	5	7+	2	10	4	7-	85.6033	0.0003	
3	12	5	8+	2	11	4	8-	86.8608	-0.0002	
3	13	5	8-	2	12	4	8+	88.1860	-0.0004	
3	13	5	9+	2	12	4	9-	88.1571	0.0003	
3	14	5	9-	2	13	4	9+	89.5213	0.0000	
3	14	5	10+	2	13	4	10-	89.4769	0.0002	
3	15	5	10-	2	14	4	10+	90.8717	-0.0003	
3	15	5	11+	2	14	4	11-	90.8072	0.0003	
3	16	5	11-	2	15	4	11+	92.2243	-0.0005	
3	16	5	12+	2	15	4	12-	92.1334	0.0006	
3	17	5	12-	2	16	4	12+	93.5613	0.0000	
3	17	5	13+	2	16	4	13-	93.4365	-0.0002	
3	18	5	13-	2	17	4	13+	94.8445	0.0004	
3	18	5	14+	2	17	4	14-	94.6944	0.0014	
3	19	5	14-	2	18	4	14+	96.5006	0.0003	
3	19	5	15+	2	18	4	15-	95.8682	0.0013	
3	20	5	15-	2	19	4	15+	97.7437	0.0002	
3	20	5	16+	2	19	4	16-	97.5540	-0.0002	
3	14	5	9-	2	14	4	11-	80.6076	0.0002	
3	14	5	10+	2	14	4	10+	80.5625	0.0005	
3	15	5	10-	2	15	4	12-	81.3180	-0.0007	
3	16	5	12+	2	16	4	12+	81.9362	-0.0011	
3	17	5	12-	2	17	4	14-	82.7288	0.0003	
3	17	5	13+	2	17	4	13+	82.6004	0.0006	
3	18	5	13-	2	18	4	15-	83.3711	-0.0003	
3	18	5	14+	2	18	4	14+	83.2134	-0.0002	
3	19	5	15+	2	19	4	15+	83.7441	0.0002	
3	20	5	16+	2	20	4	16+	84.7865	0.0003	
3	18	5	14+	1	18	8	11-	138.7427	0.0015	
3	19	5	15+	1	19	8	12-	139.1798	0.0002	
3	19	5	14-	1	19	8	11+	139.8159	-0.0012	
3	20	5	16+	1	20	8	13-	140.1276	-0.0017	
3	20	5	15-	1	20	8	12+	140.3263	0.0012	
3	21	5	17+	1	21	8	14-	140.5561	0.0024	*
3	21	5	16-	1	21	8	13+	140.8440	-0.0018	*
2	18	9	9-	2	18	4	14+	83.8459	0.0018	
2	19	9	11+	2	19	4	16-	83.8961	0.0015	
2	19	9	10-	2	19	4	15+	84.2854	0.0002	
2	20	9	12+	2	20	4	17-	84.3126	0.0002	
3	8	8	1-	2	7	7	1+	150.4796	0.0005	*
3	8	8	0+	2	7	7	0-	150.4796	0.0005	*
3	9	8	2-	2	8	7	2+	151.0960	-0.0003	
3	9	8	1+	2	8	7	1-	151.0960	-0.0003	
3	10	8	3-	2	9	7	3+	151.7173	-0.0003	
3	10	8	2+	2	9	7	2-	151.7173	-0.0003	
3	11	8	4-	2	10	7	4+	152.3466	0.0013	*
3	11	8	3+	2	10	7	3-	152.3466	0.0013	*
3	12	8	5-	2	11	7	5+	152.9807	-0.0008	
3	12	8	4+	2	11	7	4-	152.9807	-0.0008	
3	13	8	6-	2	12	7	6+	153.6276	-0.0006	
3	13	8	5+	2	12	7	5-	153.6276	-0.0006	
3	14	8	7-	2	13	7	7+	154.2876	0.0002	*
3	14	8	6+	2	13	7	6-	154.2876	0.0002	*
3	15	8	8-	2	14	7	8+	154.9605	-0.0001	*
3	15	8	7+	2	14	7	7-	154.9605	-0.0001	*
3	16	8	9-	2	15	7	9+	155.6484	-0.0007	*
3	16	8	8+	2	15	7	8-	155.6484	-0.0007	*
3	17	8	10-	2	16	7	10+	156.3541	-0.0001	*
3	17	8	9+	2	16	7	9-	156.3541	-0.0001	*
3	19	8	12-	2	18	7	12+	157.8168	0.0000	*
3	19	8	11+	2	18	7	11-	157.8168	0.0000	*
3	20	8	13-	2	19	7	13+	158.5745	-0.0005	*
3	20	8	12+	2	19	7	12-	158.5745	-0.0005	*
3	9	8	2-	2	9	7	2-	145.2349	0.0008	*
3	9	8	1+	2	9	7	3+	145.2349	0.0008	*
3	11	8	4-	2	11	7	4-	145.2001	-0.0016	*
3	11	8	3+	2	11	7	5+	145.2001	-0.0016	*
3	12	8	5-	2	12	7	5-	145.2001	-0.0002	*
3	12	8	4+	2	12	7	6+	145.2001	-0.0002	*
3	14	8	6+	2	14	7	7-	145.2349	-0.0017	*
3	14	8	6+	2	14	7	8+	145.2349	-0.0017	*
3	16	8	9-	2	16	7	9-	145.3341	-0.0004	*
3	16	8	8+	2	16	7	10+	145.3341	-0.0004	*
3	18	8	11-	2	18	7	11-	145.5016	-0.0003	*
3	18	8	10+	2	18	7	12+	145.5016	-0.0003	*
3	19	8	12-	2	19	7	12-	145.6135	0.0007	*
3	19	8	11+	2	19	7	13+	145.6135	0.0007	*
3	4	0	4	2	4	-1	4	84.7198	0.0022	
3	6	0	6	2	6	-1	6	84.7139	0.0003	
3	7	0	7	2	7	-1	7	84.8024	0.0008	
3	8	0	8	2	8	-1	8	84.9551	0.0009	
3	9	0	9	2	9	-1	9	85.1741	0.0017	
3	10	0	10	2	10	-1	10	85.4574	0.0017	
3	11	0	11	2	11	-1	11	85.8029	0.0004	
3	12	0	12	2	12	-1	12	86.2097	-0.0007	*
3	13	0	13	2	13	-1	13	86.6768	0.0003	
3	14	0	14	2	14	-1	14	87.1989	0.0010	
3	15	0	15	2	15	-1	15	87.7704	-0.0007	*
3	16	0	16	2	16	-1	16	88.3949	0.0018	
3	17	0	17	2	17	-1	17	89.0627	0.0018	
3	18	0	18	2	18	-1	18	89.7739	0.0021	
3	5	-1	4	2	4	0	4	102.4400	-0.0003	
3	6	-1	5	2	5	0	5	103.0144	0.0011	
3	7	-1	6	2	6	0	6	103.5568	0.0000	
3	8	-1	7	2	7	0	7	104.0700	-0.0012	*
3	9	-1	8	2	8	0	8	104.5598	0.0005	
3	10	-1	9	2	9	0	9	105.0271	0.0005	
3	12	-1	11	2	11	0	11	105.9320	0.0008	
3	16	-1	15	2	15	0	15	107.9225	0.0002	
3	18	-1	17	2	17	0	17	109.2008	0.0007	
3	19	-1	18	2	18	0	18	109.9472	0.0015	
3	20	-1	19	2	19	0	19	110.7720	0.0005	
3	2	-1	1	2	2	0	2	99.2542	-0.0003	*
3	4	-1	3	2	4	0	4	99.1820	-0.0008	*
3	5	-1	4	2	5	0	5	99.1031	-0.0006	*
3	7	-1	6	2	7	0	7	98.8563	-0.0005	*
3	8	-1	7	2	8	0	8	98.6901	-0.0018	*
3	9	-1	8	2	8	-2	7	112.4915	-0.0015	*
3	10	-1	9	2	9	-2	8	113.3774	-0.0012	*
3	11	-1	10	2	10	-2	9	114.2697	-0.0009	*
3	5	-1	4	2	5	-2	4	105.9462	0.0008	
3	6	-1	5	2	6	-2	5	106.1723	0.0016	
3	9	-1	8	2	9	-2	8	106.8564	-0.0014	*
3	10	-1	9	2	10	-2	9	107.0962	0.0004	
3	11	-1	10	2	11	-2	10	107.3434	0.0010	
3	12	-1	11	2	12	-2	11	107.6016	0.0012	
3	13	-1	12	2	13	-2	12	107.8739	0.0002	
3	14	-1	13	2	14	-2	13	108.1676	0.0012	
3	15	-1	14	2	15	-2	14	108.4833	0.0002	
3	16	-1	15	2	16	-2	15	108.8302	0.0013	
3	17	-1	16	2	17	-2	16	109.2098	0.0007	
3	18	-1	17	2	18	-2	17	109.6291	-0.0004	
3	19	-1	18	2	19	-2	18	110.0964	0.0008	
3	20	-1	19	2	20	-2	19	110.6135	0.0002	
3	2	-1	1	2	3	1	2	90.1325	0.0018	
3	4	-1	3	2	5	1	4	88.9092	-0.0003	
3	8	-1	7	2	9	1	8	86.5431	0.0020	
3	9	-1	8	2	10	1	9	85.9579	-0.0007	*
3	10	-1	9	2	11	1	10	85.3797	0.0008	
3	11	-1	10	2	12	1	11	84.8024	-0.0011	*
3	13	-1	12	2	14	1	13	83.6861	-0.0009	*
3	2	-1	1	2	2	2	0	87.2591	-0.0006	*
3	3	-1	2	2	3	2	1	87.4400	-0.0002	*
3	6	-1	5	2	6	2	4	88.2129	0.0015	*
3	3	-2	1	2	3	-1	3	130.5202	-0.0013	*
3	5	-2	3	2	5	-1	5	130.3616	-0.0008	*
3	6	-2	4	2	6	-1	6	130.3494	-0.0016	*
3	7	-2	5	2	7	-1	7	130.3883	-0.0006	*
3	9	-2	7	2	9	-1	9	130.6128	-0.0020	*
3	11	-2	9	2	11	-1	11	131.0290	-0.0014	*
3	4	3	2	2	4	2	2	81.1947	0.0014	
3	5	3	3	2	5	2	3	81.4521	0.0008	
3	6	3	4	2	6	2	4	81.7388	0.0016	
3	7	3	5	2	7	2	5	82.0456	0.0005	
3	10	3	8	2	10	2	8	83.0577	0.0012	*
3	3	3	1	2	2	2	0	82.7452	0.0011	
3	4	3	2	2	3	2	1	83.5743	-0.0005	
3	5	3	3	2	4	2	2	84.4502	0.0008	
3	6	3	4	2	5	2	3	85.3611	0.0018	
3	7	3	5	2	6	2	4	86.2983	0.0008	
3	9	3	7	2	8	2	6	88.2379	0.0009	
3	10	3	8	2	9	2	7	89.2307	0.0012	
3	11	3	9	2	10	2	8	90.2336	0.0016	
3	12	3	10	2	11	2	9	91.2406	0.0004	
3	4	4	1	2	3	3	0	109.4528	-0.0003	
3	5	4	2	2	4	3	1	110.1668	0.0016	*
3	6	4	3	2	5	3	2	110.9021	-0.0017	*
3	7	4	4	2	6	3	3	111.6709	0.0000	
3	8	4	5	2	7	3	4	112.4656	-0.0015	*
3	9	4	6	2	8	3	5	113.2930	0.0008	
3	10	4	7	2	9	3	6	114.1459	0.0006	
3	11	4	8	2	10	3	7	115.0257	0.0005	
3	12	4	9	2	11	3	8	115.9303	-0.0003	
3	13	4	10	2	12	3	9	116.8614	0.0014	
3	15	4	12	2	14	3	11	118.7863	0.0019	*
3	4	4	1	2	4	3	1	106.9155	-0.0010	
3	5	4	2	2	5	3	2	107.0066	0.0014	
3	6	4	3	2	6	3	3	107.1234	0.0011	
3	7	4	4	2	7	3	4	107.2667	-0.0017	*
3	8	4	5	2	8	3	5	107.4423	-0.0009	
3	11	4	8	2	11	3	8	108.1300	0.0001	
3	12	4	9	2	12	3	9	108.4091	0.0008	
3	14	4	11	2	14	3	11	109.0297	-0.0003	
3	4	4	1	2	5	5	1	91.0718	0.0005	
3	6	4	3	2	7	5	3	89.6002	0.0000	
3	7	4	4	2	8	5	4	88.8437	0.0003	
3	8	4	5	2	9	5	5	88.0708	-0.0022	*
3	9	4	6	2	10	5	6	87.2890	-0.0011	*
3	10	4	7	2	11	5	7	86.4966	0.0002	
3	11	4	8	2	12	5	8	85.6930	-0.0010	
3	12	4	9	2	13	5	9	84.8865	0.0009	
3	13	4	10	2	14	5	10	84.0725	-0.0020	*

[a]Upper and lower state quantum numbers are indicated by ' and ", respectively. Torsion-rotation levels of A species have a ± "parity" label. Those of E species have a signed K_a value. The quantum number v_t indicates the torsional state. J, K_a and K_c are the usual asymmetric rotor rotational quantum numbers. P is the parity.
[b]Measured wavenumbers in cm^{-1} from the Ottawa far-infrared BOMEM spectrum; experimental uncertainty was taken to be 0.0005 cm^{-1}.
[c]Residuals from the present fit (Tables III-VII) are given in the O-C columns in cm^{-1}. Lines with an * were excluded from the fit.

TABLE 7
Root-Mean-Square Deviations from the Global Fit of Tables 3–6

Number of parameters		57
RMS of the 1013 v_t=0-0 MW Lines		0.531 MHz
RMS of the 848 v_t=1-1 MW Lines		0.558 MHz
RMS of the 609 v_t=2-2 MW Lines		0.366 MHz
RMS of the 346 v_t=3-3 MW Lines		0.899 MHz
RMS of the 44 v_t=4-4 MW Lines		1.113 MHz
RMS of the 464 v_t=1-0 FIR Lines		0.00042 cm^{-1}
RMS of the 417 v_t=2-1 FIR Lines		0.00051 cm^{-1}[a]
RMS of the 224 v_t=3-2 FIR Lines		0.00074 cm^{-1}[a]

Lines[b]	Uncertainty[c]	RMS[d]	Lines[b]	Uncertainty[c]	RMS[d]
11	0.004-0.005	2.9	387	0.080	1.2
2	0.010	0.8	6	0.100	0.6
60	0.020	1.8	60	0.130-0.200	1.3
494	0.030-0.050	1.1	1339	1.0	0.8
501	0.070	1.8			

[a]The far-infrared hot-band lines were given an uncertainty √2 times larger that the v_t=1-0 lines, i.e., an uncertainty of 0.00050 cm^{-1}, to allow for expected, but difficult to detect, blending with lines of the fundamental band.
[b]Number of MW lines in each uncertainty group.
[c]Experimental uncertainty range in MHz for each group.
[d]Dimensionless root-mean-square weighted deviation for each group, which would be 1.0 if the fit were good to experimental uncertainty.

ing analyzed a number of the $v_t = 3$ levels, we can now locate candidates for a large number of transitions involving these perturbed levels, both in the millimeter and in the far-infrared region. Some of these lines have been included in our final fit and some have not, reflecting the fact that the present treatment of these perturbed regions is still provisional.

Consider as an example the $v_t = 2$ levels of $A\pm$ species with $K = 9$. The perturbing states are found to be $v_t = 3$, $K = 5$, $A\mp$, with an interaction matrix element of some 7.5 GHz at the avoided crossing near $J = 19$. The corresponding energy levels are illustrated in Fig. 5, where $B_{\text{eff}} J(J + 1)$ with $B_{\text{eff}} = 0.3324\ \text{cm}^{-1}$ has been subtracted from the actual energies. Solid lines connecting energy levels in this figure indicate observed submillimeter transitions with residuals less than 2 MHz in our global fit; dashed lines indicate transitions with residuals between 2 and 10 MHz. (Many of the dashed lines correspond to ''forbidden'' transitions made allowed by mixings induced by this perturbation.) Table 8 gives observed minus calculated residuals and calculated relative intensities for a number of infrared and microwave transitions involving these levels, most of which were excluded from the fit because their assignment and/or degree of blending is not completely certain.

An avoided crossing of similar magnitude was also found for $v_t = 2$ levels of E species with $K = -9$, as shown in Fig. 6. In this case the interacting partner is $v_t = 3$, $K = -6$, with an interaction matrix element of magnitude 7.5 GHz at the avoided crossing near $J = 16$.

Careful studies based on preliminary analyses like those illustrated above are now feasible for a number of avoided crossing regions. Such studies should lead to precise values for various torsion–rotation interaction terms, which after reconciliation with those obtained from high-level *ab initio* calculations at various torsional angles (*18–21*) can ultimately be used in attempts to elucidate intramolecular energy flow pathways. Such studies may also shed light on the legitimacy of reduced torsion–rotation Hamiltonians (*17, 22, 23*) when strongly avoided crossings are present in an energy level system.

Some systematization of torsion-rotation interactions like those illustrated in Figs. 5 and 6 is possible using symmetry considerations (*6*). For levels of A species there are two kinds of terms controlling the $\Delta v_t = 1$ perturbations under discussion here. One type,

$$\sin 3n\gamma(P_aP_c + P_cP_a)$$
$$\sin 3n\gamma(P_bP_c + P_cP_b), \qquad [7]$$

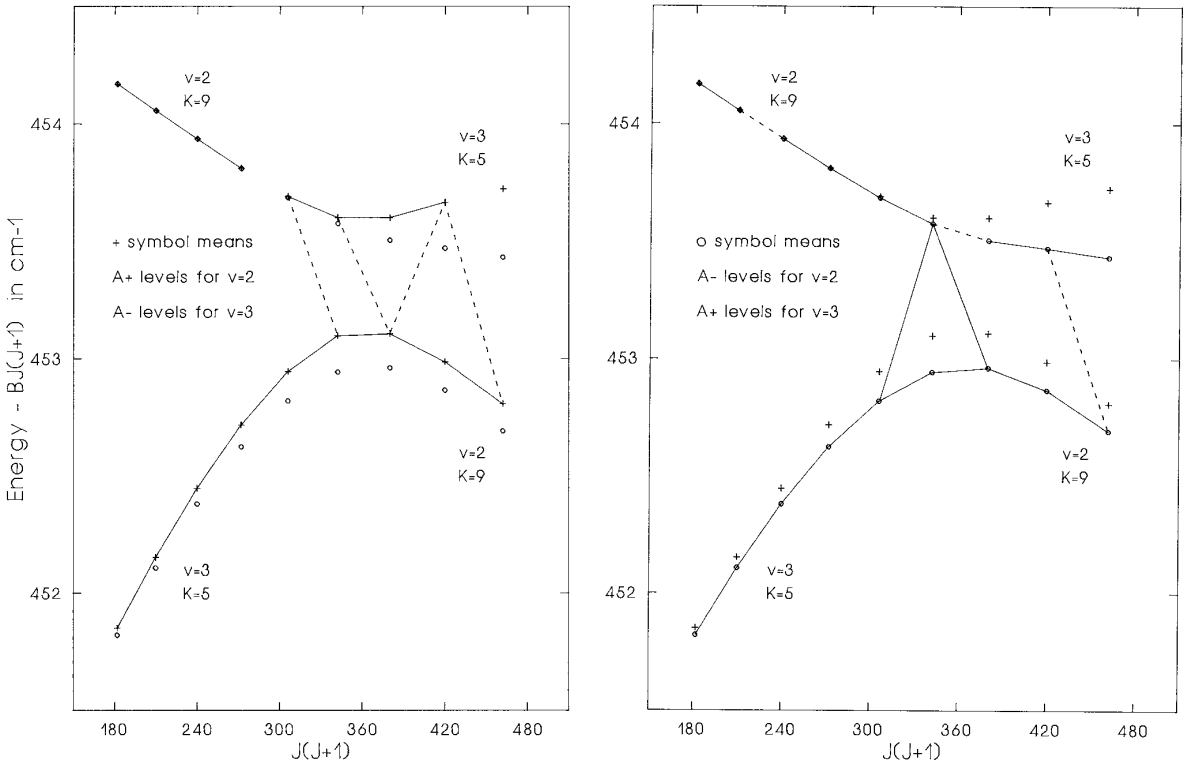

FIG. 5. The avoided crossing between $v_t = 2$, $K = 9$, $A\pm$ and $v_t = 3$, $K = 5$, $A\mp$ levels. Energies for levels with $13 \leqslant J \leqslant 21$ are plotted after subtracting $B_{\text{eff}} J(J+1) = (0.3324)J(J+1)$, so that slopes at the crossing are nearly horizontal. The same $A\pm$ energy level points are plotted in the left and right panels of this figure. Observed transitions with residuals in our global fit less than 2 MHz are indicated by solid lines, in the left panel for the interacting $v_t = 2$, $A+$ and $v_t = 3$, $A-$ levels, and in the right panel for the interacting $v_t = 2$, $A-$ and $v_t = 3$, $A+$ levels. Tentatively assigned transitions in the two panels, with residuals between 2 and 10 MHz, are indicated by dashed lines. Unobserved or badly blended lines are indicated by missing connections between points. The maximum energy level displacement due to the interaction between these $v_t = 2$ and $v_t = 3$ levels is about 7.5 GHz = 0.25 cm^{-1}. Note that with the v_t, K labeling scheme used in our global fit program, the upper (lower) curve on the left contains $v_t = 2$, $K = 9+$ ($v_t = 3$, $K = 5-$) energy levels with J from 13 to 18, and $v_t = 3$, $K = 5-$ ($v_t = 2$, $K = 9+$) energy levels with J from 19 to 21. The upper (lower) curve on the right contains $v_t = 2$, $K = 9-$ ($v_t = 3$, $K = 5+$) energy levels with J from 13 to 19, and $v_t = 3$, $K = 5+$ ($v_t = 2$, $K = 9-$) energy levels with $J = 20$ and 21. Intensities calculated from the fit program for a number of observed and unobserved transitions between these interacting levels are given in Table 8.

involves the torsional operators $\sin 3n\gamma$, $n = 1, 2, 3, \ldots$, which are of species A_2 and invariant to time reversal. The other type,

$$P_\gamma^{2n+1}(P_a + P_a^3 + P_a^5 + \cdots), \qquad [8]$$

involves the torsional operators P_γ^{2n+1}, which are also of species A_2, but which go into their negatives under time reversal. Table 1 indicates that interactions between $v_t = 2$ and $v_t = 3$ A levels involve a formal change of m from 3 to 6, so that operators with the value $n = 1$ in Eq. [7], corresponding to the parameters D_{ac} and D_{bc} in our program (see Table 3), are expected to be the main contributors to perturbations between these two torsional levels. It is more difficult to guess which operators in Eq. [8] will contribute most to such perturbations, but those with $n = 0$ correspond to the parameters ρ, k_1, and l_k, respectively, the first operator with $n = 1$ corresponds to k_3, and the first with $n = 2$ corresponds to k_{3B} in our program and Table 3.

Symmetry considerations for E species are more complicated, and lead to the conclusion that the $\Delta v_t = 1$ perturbations under discussion can be caused by four types of operators. The first two types are identical to those given in Eqs. [7] and [8] above. The third type,

$$\cos 3n\gamma(1 + P^2 + P_a^2 + \cdots), \qquad [9]$$

involves the A_1 torsional potential operators $\cos 3n\gamma$, which go into themselves under time reversal. The fourth type,

$$P_\gamma^{2n}(1 + P^2 + P_a^2 + \cdots), \qquad [10]$$

involves A_1 torsional momentum operators P_γ^{2n} which also go into themselves under time reversal. Table 1 indicates

TABLE 8

Calculated Frequencies and Intensities for Some Observed and Unobserved Lines in the Avoided Crossing Region of the $v_t = 2$, $K = 9$ and $v_t = 3$, $K = 5$ $A\pm$ levels

Allowed and Forbidden Submillimeter Transitions[a]

v_t'J'K_a'	v_t"J"K_a"	ν_{obs}[b]	ν_{calc}[c]	O-C[c]		I_c[c]	I_o[d]	v_t'J'K_a'	v_t"J"K_a"	ν_{obs}[b]	ν_{calc}[c]	O-C[c]		I_c[c]	I_o[d]
2 14 9+	2 13 9+	275606.1	275606.6	-0.5	* M	4.1	6.6	2 14 9-	2 13 9-	275606.1	275605.7	0.4	* M	4.1	6.6
2 15 9+	2 14 9+	295335.9	295337.1	-1.2	* M	4.6	5.2	2 15 9-	2 14 9-	295335.9	295332.7	3.2	* M	4.6	5.2
2 16 9+	2 15 9+	315142.1	315142.6	-0.5	V	5.0		2 16 9-	2 15 9-		315120.5	-0.0	M	5.0	
2 17 9+	2 16 9+		335188.4			5.2		2 17 9-	2 16 9-		335072.8	335071.5	1.2	X	5.3	5.4
2 18 9+	2 17 9+	356065.5	356066.4	-0.9	X	5.3	4.9	2 18 9-	2 17 9-	355442.3	355442.4	-0.1	X	5.4	4.2
3 19 5-	2 18 9+	378654.9	378654.7	0.2	* X	5.2	4.4	2 19 9-	2 18 9-		376535.0	376538.5	-3.5	* X	5.5	3.2
3 20 5-	3 19 5-	400587.1	400587.0	0.1	* X	5.9	5.1	3 20 5+	2 19 9-	397604.4	397604.2	0.2	* X	5.8	3.4
3 21 5-	3 20 5-		420263.4			6.2		3 21 5+	3 20 5+	417373.0	417374.3	-1.2	* X	6.1	4.2
3 14 5-	3 13 5-	288105.2	288104.8	0.4	X	5.7	4.3	3 14 5+	3 13 5+	287651.2	287650.4	0.8	* X	5.7	4.2
3 15 5-	3 14 5-	307739.7	307739.9	-0.2	V	6.0	5.6	3 15 5+	3 14 5+	307120.0	307120.1	-0.1	V	6.0	6.1
3 16 5-	3 15 5-	326983.9	326984.1	-0.2	X	6.1	6.6	3 16 5+	3 15 5+	326165.1	326164.8	0.4	X	6.1	3.0
3 17 5-	3 16 5-	345692.9	345692.4	0.5	X	6.2	9.7	3 17 5+	3 16 5+	344695.9	344694.8	1.1	X	6.2	6.8
3 18 5-	3 17 5-	363294.2	363294.0	0.2	X	6.0	6.3	3 18 5+	3 17 5+	362471.0	362470.5	0.5	X	6.2	6.0
2 19 9+	3 18 5-	378935.8	378935.2	0.6	* X	5.5	4.9	3 19 5+	3 18 5+	379212.1	379212.0	0.1	X	6.0	4.6
2 20 9+	2 19 9+	395009.8	395010.8	-1.1	X	5.8	4.7	2 20 9-	3 19 5+	395711.2	395711.8	-0.6	* X	6.0	3.7
2 21 9+	2 20 9+	413153.7	413153.7	0.0	X	6.0	3.8	2 21 9-	2 20 9-	413283.3	413284.0	-0.6	X	6.1	3.1
3 17 5-	2 16 9+		312896.7			0.0		3 17 5+	2 16 9-		309141.6			0.0	
3 18 5-	2 17 9+	340998.6	341002.3	-3.7	* X	0.3	0.7	3 18 5+	2 17 9-		336540.6			0.1	
2 19 9+	2 18 9+	363877.5	363871.1	6.4	* X	0.6	0.4	3 19 5+	2 18 9-	360308.2	360310.2	-1.9	* X	0.2	7.6
2 20 9+	3 19 5-		380227.2			0.2		2 20 9-	2 19 9-		379483.5			0.2	
2 21 9+	3 20 5-	392784.7	392793.8	-9.1	* X	0.0	6.6	2 21 9-	3 20 5+	395155.7	395163.3	-7.6	* X	0.0	1.2
2 17 9+	3 16 5-		367984.2			0.1		2 17 9-	3 16 5+		370624.8			0.0	
2 18 9+	3 17 5-		378358.2			0.4		2 18 9-	3 17 5+	381372.4	381372.4	0.0	* X	0.2	0.7
3 19 5-	3 18 5-		393718.9			0.8		2 19 9-	3 18 5+	395461.4	395440.4	21.0	* X	0.4	2.9
3 20 5-	2 19 9+	415380.4	415370.7	9.7	* X	0.3	1.1	3 20 5+	3 19 5+		413832.5			0.3	
3 21 5-	2 20 9+		440623.2			0.1		3 21 5+	2 20 9-		435494.9			0.1	

Allowed and Forbidden Infrared Transitions[e]

v_t'J'K_a'	v_t"J"K_a"	ν_{obs}[f]	O-C[c]		v_t'J'K_a'	v_t"J"K_a"	ν_{obs}[f]	O-C[c]		v_t'J'K_a'	v_t"J"K_a"	ν_{obs}[f]	O-C[c]	
2 9 9-	1 9 8-	137.5375	0.0002	*	2 10 9+	1 9 8+	144.1025	-0.0001	*	3 14 8-	2 15 9+	93.4365	-0.0023	*
2 9 9+	1 9 8+	137.5375	0.0002	*	2 12 9-	1 11 8-	145.7132	-0.0001	*	3 14 8+	2 15 9-	93.4365	-0.0025	*
2 10 9-	1 10 8-	137.6783	-0.0004	*	2 12 9+	1 11 8+	145.7132	-0.0001	*	3 15 8-	2 16 9+	92.6525	0.0018	*
2 10 9+	1 10 8+	137.6783	-0.0004	*	2 13 9-	1 12 8-	146.5398	-0.0003	*	3 15 8+	2 16 9-	92.6525	0.0009	*
2 11 9-	1 11 8-	137.8348	0.0004	*	2 13 9+	1 12 8+	146.5398	-0.0003	*	3 16 8-	2 17 9+	91.8417	-0.0002	*
2 11 9+	1 11 8+	137.8348	0.0004	*	2 14 9-	1 13 8-	147.3814	0.0001	*	3 16 8+	2 17 9-	91.8481	0.0014	*
2 12 9-	1 12 8-	138.0039	-0.0002	*	2 14 9+	1 13 8+	147.3814	0.0001	*	3 17 8-	2 18 9+	91.0145	0.0300	*
2 12 9+	1 12 8+	138.0039	-0.0002	*	2 15 9-	1 14 8-	148.2371	-0.0005	*	3 17 8+	3 18 5+	91.6392	-0.0014	*
2 13 9-	1 13 8-	138.1885	0.0004	*	2 15 9+	1 14 8+	148.2371	-0.0007	*	3 18 8+	3 19 5+	90.6588	0.0000	*
2 13 9+	1 13 8+	138.1885	0.0004	*	2 16 9-	1 15 8-	149.1113	0.0003	*	3 9 8-	2 9 9+	103.7866	-0.0003	*
2 14 9-	1 14 8-	138.3862	-0.0002	*	2 16 9+	1 15 8+	149.1113	-0.0006	*	3 9 8+	2 9 9-	103.7866	-0.0003	*
2 14 9+	1 14 8+	138.3862	-0.0002	*	2 17 9-	1 16 8-	150.0073	0.0005	*	3 12 8-	2 12 9+	103.5141	-0.0003	*
2 15 9-	1 15 8-	138.5999	0.0002	*	2 17 9+	1 16 8+	150.0112	-0.0005	*	3 12 8+	2 12 9-	103.5141	-0.0003	*
2 15 9+	1 15 8+	138.5999	0.0000	*	2 18 9-	1 17 8-	150.9395	0.0005	*	3 13 8-	2 13 9+	103.4061	-0.0013	*
2 16 9-	1 16 8-	138.8302	0.0001	*	3 18 5-	1 17 8-	150.4632	0.0010	*	3 13 8+	2 13 9-	103.4061	-0.0013	*
2 16 9+	1 16 8+	138.8302	-0.0008	*	2 18 9+	1 17 8+	150.9637	-0.0010	*	3 14 8-	2 14 9+	103.2892	-0.0004	*
2 17 9-	1 17 8-	139.0828	0.0001	*	2 19 9-	1 18 8-	151.9314	-0.0002	*	3 14 8+	2 14 9-	103.2892	-0.0004	*
2 17 9+	1 17 8+	139.0875	-0.0001	*	2 19 9+	1 18 8+	151.5352	0.0005	*	3 15 8-	2 15 9+	103.1600	-0.0028	*
2 18 9-	1 18 8-	139.3705	-0.0012	*	2 21 9-	1 20 8-	153.3107	-0.0001	*	3 15 8+	2 15 9-	103.1600	-0.0029	*
3 18 5+	1 18 8-	138.7427	0.0015		2 22 9-	1 21 8-	154.2131	0.0009	*	3 18 5-	2 18 4-	83.3711	-0.0003	
2 18 9+	1 18 8+	139.3963	-0.0010	*	2 22 9+	1 21 8+	154.3423	0.0000	*	3 18 5+	2 18 4+	83.2134	-0.0002	
2 19 9-	1 19 8-	139.7202	-0.0007	*	3 8 8-	2 9 9+	97.9477	-0.0040	*	2 18 9-	2 18 4+	83.8459	0.0018	
3 19 5+	1 19 8-	139.1798	0.0002		3 8 8+	2 9 9-	97.9477	-0.0040	*	2 19 9+	2 19 4-	83.8961	0.0015	
3 19 5-	1 19 8+	139.8159	-0.0012		3 9 8-	2 10 9+	97.2220	0.0004	*	3 19 5+	2 19 4+	83.7441	0.0002	
3 20 5+	1 20 8-	140.1276	-0.0017		3 9 8+	2 10 9-	97.2220	0.0004	*	2 19 9-	2 19 4+	84.2854	0.0002	
3 20 5-	1 20 8+	140.3263	0.0012		3 10 8-	2 11 9+	96.4848	0.0019	*	2 20 9+	2 20 4-	84.3126	0.0002	
2 20 9+	1 20 8+	139.6457	-0.0002	*	3 10 8+	2 11 9-	96.4848	0.0019	*	3 20 5+	2 20 4+	84.7865	0.0003	
3 21 5+	1 21 8-	140.5561	0.0024	*	3 11 8-	2 12 9+	95.7389	0.0033	*	3 18 5-	2 17 4+	94.8445	0.0004	
3 21 5-	1 21 8+	140.8440	-0.0018	*	3 11 8+	2 12 9-	95.7389	0.0033	*	3 18 5+	2 17 4-	94.6944	0.0014	
2 21 9+	1 21 8+	139.9295	0.0000	*	3 12 8-	2 13 9+	94.9744	-0.0051	*	3 19 5-	2 18 4+	96.5006	0.0003	
2 9 9-	1 8 8-	143.3185	-0.0001	*	3 12 8+	2 13 9-	94.9744	-0.0051	*	3 19 5+	2 18 4-	95.8682	0.0013	
2 9 9+	1 8 8+	143.3185	-0.0001	*	3 13 8-	2 14 9+	94.2165	0.0023	*	3 20 5-	2 19 4+	97.7437	0.0002	
2 10 9-	1 9 8-	144.1025	-0.0001	*	3 13 8+	2 14 9-	94.2165	0.0023	*	3 20 5+	2 19 4-	97.5540	-0.0002	

[a] Allowed transitions have calculated intensities $I_c > 4$ and correspond mostly to solid lines in Fig. 5. Forbidden transitions have $I_c < 1$ and occur across the avoided crossings in Fig. 5. Note the abrupt quantum number change $v_t = 2$, $K = 9 \leftrightarrow v_t = 3$, $K = 5$ in the avoided crossing region. All *'d transitions were excluded from the fit.

[b] Measurements and observed minus calculated (O-C) values in MHz. Measurement sources: X = Nizhny Novgorod RAD-3, with assigned uncertainty of 1 MHz; M = Nizhny Novgorod RAD-2 and V = Lille, with assigned uncertainty of 70 kHz.

[c] From the global fit of Tables III-VII. I_c gives the Boltzmann factor at 296 K times the line strength, i.e., gives calculated "relative intensities" without the frequency and population-difference factors (see footnote d).

[d] I_o gives observed intensities from the RAD-3 charts. Since RAD-3 spectra were recorded in many separate segments, with intensities of each segment adjusted for chart paper size, precise numerical intercomparison of I_o values is not meaningful. Further, since recording in segments greatly suppresses the approximate ν^2 increase of absolute intensities of the submillimeter transitions, some ν-dependence was also removed from I_c (see footnote c).

[e] Calculated intensities are not given for allowed and forbidden infrared transitions since relative contributions of the μ_a and μ_b permanant dipole moment components and the μ_c dipole derivative are not known.

[f] Measurements (from the Ottawa BOMEM spectrum) and O-C values in cm^{-1}; *'d transitions were excluded from the fit.

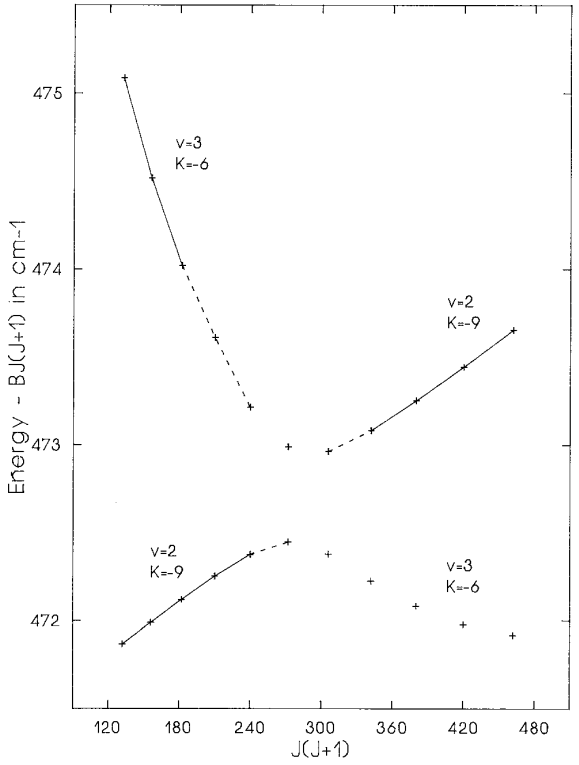

FIG. 6. The avoided crossing between $v_t = 2$, $K = -9$, E and $v_t = 3$, $K = -6$, E levels. Energies for levels with $11 \leqslant J \leqslant 21$ are plotted after subtracting $(0.3084)J(J + 1)$; observed transitions with residuals in our global fit less than 2 MHz are indicated by solid lines; tentatively assigned transitions, with residuals between 2 and 10 MHz, are indicated by dashed lines; unobserved or badly blended lines, are indicated by missing connections between points. The maximum energy displacement due to the interaction between these $v_t = 2$ and $v_t = 3$ levels is (as in Fig. 5 also) about 7.5 GHz = 0.25 cm^{-1}. With the v_t, K labeling scheme used in our global fit program, the upper (lower) set of points contains $v_t = 3$, $K = -6$ ($v_t = 2$, $K = -9$) energy levels with J from 11 to 16, and $v_t = 2$, $K = -9$ ($v_t = 3$, $K = -6$) energy levels with J from 17 to 21.

that symmetry-allowed interactions between $v_t = 2$ and $v_t = 3$ E levels must involve a formal change in m from ± 4 to ∓ 5, i.e., $\Delta m = \pm 9$, so that operators with $n = 3$ in Eqs. [7], which are not yet included in our program, or $n = 3$ in Eq. [9], of which only V_9 is in the program, are expected to be the main contributors to the perturbations. The three operators with $n = 1$ in Eq. [10] correspond to the parameters F, G_v, and k_2 in Table 3; those with $n = 2$ correspond to k_4, M_v, and K_1.

Note that the ''$\Delta v_t = 1$'' perturbations discussed separately above for torsional A and E levels are not as different as they appear. Because of the close proximity of the $v_t = 3$ A_2 and $v_t = 4$ A_1 states, and because of the $P_\gamma P_a$ Coriolis term in the Hamiltonian, there is extensive mixing of these torsional A_2 and A_1 states for $K > 0$. The nominal $\Delta v_t = 1$ perturbations in the A levels can thus also arise from $\Delta v_t = 2$ matrix elements; i.e., perturbations in A levels with $K > 0$ can also be caused by the various operators in Eqs. [9] and [10].

Many of the higher-order ''perturbation'' terms discussed above were already included in our earlier fits (*1–5*). Thus, once transitions to $v_t = 3$ levels were added to the data set, calculations for lines in the perturbed K subbranches in $v_t = 2$ improved significantly. It is quite pleasing to note that the present model can handle these various torsion–rotation interactions in a relatively satisfactory way, but it is also necessary to point out that a number of the terms described above and included in our Hamiltonian are forbidden within the reduced Hamiltonian model (*17, 22, 23*). It is not clear at present, whether (i) these fourth-order terms should be strictly eliminated from our fit, or (ii) inclusion of these terms becomes necessary because of avoided crossings and their associated ''near zero energy denominators,'' or (iii) some change in the original rotational and torsional operator ordering scheme (which assumes, for example, that $\frac{1}{2}V_3(1 - \cos 3\gamma)$ and BJ_x^2 are both of order 2), needs to be considered for the case of acetaldehyde.

B. $\Delta K = 0$ Interactions near Avoided Crossings of the Parabolas

The energy levels shown in Figs. 1–3 were obtained from the Hamiltonian H_{tKr} in Eq. [1], which corresponds closely to the Hamiltonian used in the first of the two diagonalization steps in our present computer program (*1–5*). (The first step in the program also includes the potential terms $\cos 6\gamma$, $\cos 9\gamma$ and $\cos 12\gamma$, but does not include $[A - (B + C)/2]K^2$.) H_{tKr} takes into account four physical phenomena: (i) the kinetic energy FP_γ^2 associated with internal rotation, (ii) the potential energy $(1/2)V_3(1 - \cos 3\gamma)$ associated with internal rotation, (iii) the kinetic energy $[A - (B + C)/2 + F\rho^2]K^2$ associated with overall rotation of the molecule about a z-axis chosen to lie along the ρ vector (*6*) in the molecule, and (iv) the Coriolis interaction $+2F\rho P_\gamma J_z$ between internal rotation and overall rotation. Furthermore, H_{tKr} commutes with J_z (called P_a in Table 3), so the signed value of K is a good quantum number for eigenvectors of H_{tKr}. The term in K^2 from (iii) above thus represents a simple additive constant for all eigenvalues of given K, and it could therefore be omitted in any discussion of purely $\Delta K = 0$ interactions. Its contribution is included in the energy levels plotted in Figs. 1–3, but the $[A - (B + C)/2]K^2$ portion is excluded from the energies in Fig. 4.

We turn now to three empirical patterns which emerge from the numerical eigenvalue and eigenvector calculations for acetaldehyde levels with $K \leqslant 20$. These patterns are easily described using the signed m labels in Fig. 3, which indicate the free-rotor basis function $e^{+im\gamma}$ contributing most to each final eigenstate for various positive values of K.

First, the $m > 0$ levels (using the sign convention of Eq.

TABLE 9

Basis Set Coefficients for a Range of m Values,[a] Taken from Column Eigenvectors of H_{tor} in Eq. [1] for Various Values of the Good Quantum Number K, Illustrating the $m \rightarrow m + 9$ Labeling Change[b] for Energy Levels in Fig. 3 Which Pass through a Minimum as K Changes

	m = -5 → m = +4					
m/K	-1	0	1	2	3	4
-8	-0.29	-0.28	-0.26	-0.20	-0.14	-0.12
-5	-0.76	-0.69	-0.56	-0.35	-0.18	-0.09
-2	+0.50	+0.53	+0.52	+0.44	+0.33	+0.25
+1	-0.25	-0.33	-0.44	-0.52	-0.53	-0.50
+4	+0.09	+0.18	+0.34	+0.55	+0.69	+0.76
+7	+0.12	+0.14	+0.20	+0.26	+0.28	+0.29

	m = -7 → m = +2					
m/K	5	6	7	8	9	10
-10	-0.29	-0.29	-0.26	-0.20	-0.15	-0.13
-7	-0.76	-0.70	-0.57	-0.37	-0.19	-0.10
-4	+0.50	+0.53	+0.53	+0.45	+0.34	+0.26
-1	-0.24	-0.32	-0.43	-0.52	-0.53	-0.51
+2	+0.08	+0.17	+0.33	+0.54	+0.68	+0.75
+5	+0.12	+0.14	+0.19	+0.25	+0.28	+0.29

	m = -6 → m = +3					
m/K	2	3	4	5	6	7
-9	-0.29	-0.28	-0.26	-0.20	-0.15	-0.12
-6	-0.76	-0.69	-0.56	-0.36	-0.19	-0.09
-3	+0.50	+0.53	+0.52	+0.45	+0.34	+0.25
0	-0.25	-0.33	-0.43	-0.52	-0.53	-0.50
+3	+0.08	+0.18	+0.33	+0.54	+0.68	+0.76
+6	+0.12	+0.14	+0.19	+0.26	+0.28	+0.29

	m = -8 → m = +1					
m/K	8	9	10	11	12	13
-11	-0.29	-0.29	-0.26	-0.21	-0.15	-0.13
-8	-0.77	-0.70	-0.58	-0.37	-0.20	-0.10
-5	+0.50	+0.53	+0.53	+0.45	+0.34	+0.26
-2	-0.24	-0.32	-0.42	-0.52	-0.53	-0.51
+1	+0.08	+0.17	+0.32	+0.53	+0.67	+0.75
+4	+0.12	+0.14	+0.19	+0.25	+0.28	+0.29

[a] Note that numerical entries in the four individual blocks in this table are nearly identical. This is a consequence of the facts that: (i) the transformation m → m-1 and K → K+3 leaves H_{tor} in Eq. (1) invariant when $\rho = 1/3$, and (ii) $\rho \approx 1/3$ for CH_3CHO.

[b] The transformation m → -m, K → -K can be used together with the transformation above to show, for example, that entries read from the top down in the K = -1, 0 and 1 columns of the m = -5 table have the same magnitude as entries read from the bottom up in the K = 4, 3 and 2 columns of the m = -5 table, respectively.

[4] and positive K values) show rather simple behavior in Fig. 3, since they increase in energy rather smoothly with K and preserve their m quantum number. Qualitatively, this behavior agrees with that expected theoretically from the free-rotor energy expression $F(m + \rho K)^2 + [A - (B + C)/2]K^2$ when $mK > 0$. Unfortunately, simply adding $E^{(2)}(m, K)$ from Eq. [5] to the free-rotor energies does not lead to more quantitative agreement because the perturbation treatment often fails when $K \geqslant 2$.

Second, the $m < 0$ levels first decrease in energy with K and then increase. This is the qualitative behavior expected from the free-rotor energy expression when $mK < 0$ and $F \gg [A - (B + C)/2]$. Somewhat more difficult to understand is the fact that just after the minimum energy K value, the $m < 0$ levels change their m quantum number rather abruptly from m to $m + 9$, as shown by the basis function coefficients in Table 9. Coefficients for the four examples in Table 9 are nearly identical because the transformation $m \rightarrow m - 1$, $K \rightarrow K + 3$ leaves H_{tor} in Eq. [1] invariant if $\rho = 1/3$. This transformation together with $m \rightarrow -m$, $K \rightarrow -K$, which also leaves H_{tor} invariant, can be used to show that the eigenfunction coefficients A_m^K (*7, 15*) obey the relations $|A^1_{-5}| = |A^2_{+4}| = |A^4_{-6}| = |A^5_{+3}| = |A^7_{-7}| = |A^8_{+2}|$, etc. Thus, when $\rho = 1/3$, (i) an eigenfunction which is mainly $m = -5$ for $K = 1$ must become mainly $m = +4$ for $K = 2$, an eigenfunction which is mainly $m = -6$ for $K = 4$ must become mainly $m = +3$ for $K = 5$, etc., and (ii) the magnitudes of the coefficients involved in all of these sudden m quantum number changes must be the same. These two observations provide a partial after-the-fact explanation for the eigenvector behavior displayed in Table 9.

Third, when levels of different m and the same symmetry (same m mod 3) cross because one set of levels decreases in energy with K while the other set increases, then some wavefunction mixing and mutual repulsion occurs, as shown in Table 10. It turns out that K values for the $\Delta K = 0$ avoided crossings above the barrier in acetaldehyde can be calculated rather well from the free-rotor energies formally corrected to second order for barrier effects, i.e., can be calculated by setting

$$F(m_1 + \rho K)^2 + E^{(2)}(m_1, K) + [A - (B + C)/2]K^2 = F(m_2 + \rho K)^2 + E^{(2)}(m_2, K) + [A - (B + C)/2]K^2 \qquad [11]$$

and noting (see Eq. [5]) that this equality is satisfied when

$$(m_1 + \rho K)^2 = (m_2 + \rho K)^2. \qquad [12]$$

By taking square roots of opposite sign on the left and right of Eq. [12], a crossing for two levels of the same symmetry is predicted when

TABLE 10
Basis Set Coefficients Illustrating Wavefunction Mixing[a] near the $m = +5$ and $m = -7$ Avoided Crossing Circled at $K = 3$ in Figs. 3 and 4

|m = +5>						|m = -7>					
m/K	1	2	3	4	5	m/K	1	2	3	4	5
-13	+0.00	+0.00	+0.02	-0.00	-0.00	-13	-0.03	-0.03	-0.03	-0.04	-0.04
-10	+0.03	+0.04	+0.18	-0.03	-0.02	-10	-0.26	-0.26	-0.20	-0.28	-0.29
-7	+0.12	+0.15	+0.57	-0.08	-0.03	-7	-0.87	-0.84	-0.61	-0.80	-0.76
-4	+0.09	+0.02	-0.26	+0.09	+0.05	-4	+0.40	+0.42	+0.37	+0.46	+0.50
-1	-0.25	-0.18	-0.02	-0.16	-0.13	-1	-0.13	-0.16	-0.23	-0.18	-0.24
+2	+0.50	+0.47	+0.31	+0.42	+0.40	+2	+0.05	+0.08	+0.32	+0.01	+0.08
+5	-0.76	-0.80	-0.66	-0.84	-0.87	+5	-0.02	-0.07	-0.52	+0.16	+0.12
+8	-0.29	-0.28	-0.21	-0.26	-0.26	+8	-0.02	-0.03	-0.17	+0.04	+0.03
+11	-0.04	-0.04	-0.03	-0.03	-0.03	+11	-0.00	-0.00	-0.02	+0.00	+0.00

[a]For K = 1,2,4,5 the nominal |m=+5> and |m=-7> eigenfunctions contain mainly the m=+5 and m=-7 basis functions, respectively. At the K = 3 avoided crossing these eigenfuctions contain large amounts of both the m=+5 and m=-7 basis functions.

$$m_1 + m_2 = -2\rho K$$
$$m_1 - m_2 = 0 \bmod 3. \qquad [13]$$

K values calculated for avoided crossings when $\rho = 1/3$ are given in Table 11. These can be seen to agree well with K values for the acetaldehyde avoided crossings shown in the circled regions in Figs. 3 and 4.

As discussed in connection with Table 2, the second order perturbation expression $E^{(2)}(m, K)$ given in Eq. [5] and used in Eq. [11] will diverge for many sets of m_1, m_2, K values. Nevertheless, this expression, and therefore Eqs. [12] and [13], are expected to be valid for $K = 0$ and 1 and $m \geqslant 5$, i.e., are expected to be valid for avoided crossings in the last three rows of the $K = 0$ column in Table 11. Equations [12] and [13] are also valid, however, for the other avoided crossings above the barrier in Table 11, because (i) the low-K corrections $E^{(2)}(m, K)$ are functions only of $(m + \rho K)^2$, and (ii) second-order corrections for other m_1, m_2, K sets, while not obtainable by direct substitution in Eq. [5], can be obtained from the transformation $K \rightarrow K + 3$, $m \rightarrow m - 1$, which leaves $(m + \rho K)^2$ invariant when $\rho = 1/3$. The ''true'' second-order corrections to the free-rotor energies are thus also functions only of $(m + \rho K)^2$, which is sufficient to make the derivation of Eqs. [12] and [13] correct for all m_1, m_2, K values.

C. $\Delta K \neq 0$ Interactions near Minima of the Parabolas

In an ordinary asymmetric rotor molecule without internal rotation, the largest $\Delta K \neq 0$ mixings (which obey also ΔK = even) occur at low K where $\Delta K \neq 0$ energy differences are smallest. Figure 2 indicates that for torsional energy levels above the barrier, near degeneracies of different K levels occur near the minima of the various parabolas. For the present problem we thus expect large $\Delta K \neq 0$ mixings (both ΔK = even and ΔK = odd) among K values near these minima. Indeed, rather large fluctuations in calculated transition frequencies as a function of changes in the parameter and/or data set are observed in our fits for $v_t = 3$ and 4 levels near the minima of the parabolas, which together with the associated K-labeling problems, often make unambiguous line assignments difficult or impossible. Unexpectedly, mutual repulsions resulting from these mixings seem particularly important for levels with $J \sim K$. This is illustrated in Table 12 by the anomalously large or small effective B values obtained near $J = K$ when acetaldehyde energy eigenvalues obtained from our final global fit are substituted into the expression

$$B_{\text{eff}}(J + 1, K) = [E(J + 1, K) - E(J, K)]/(2J + 2). \qquad [14]$$

D. K Quantum Number Labeling Problems

The problem of finding a correct and/or unique K label for the eigenvectors of all states involved in the fit (5) still remains in the present work. A rotational energy surface study (*24*) suggested that most of the K labeling problems could be removed by redefining the K quantum number as the projection of J along a z axis chosen to pass through a suitable maximum of the rotational energy surface, but for reasons we do not yet understand, implementation of such ideas in our program did not remove all problems in practice. As a result, the K labeling scheme used in this present fit must still be considered to be empirical, in the sense that the final criteria imposed were (i) the K value for a given series of rotational energy levels is defined by the lowest

TABLE 11
Avoided Crossings in Fig. 3, as Calculated from Eqs. [13]

K =	0	3	6	9	12	Note
m_1,m_2	+3,-3	+2,-4	+1,-5	0,-6	-1,-7	a
	+6,-6	+5,-7	+4,-8	+3,-9	+2,-10	b
	+9,-9	+8,-10	+7,-11	+6,-12	+5,-13	c
	+12,-12	+11,-13	+10,-14	+9,-15	+8,-16	c

[a]Avoided crossings in the first row do not occur in Fig. 3, because one or both levels are below the barrier.
[b]Avoided crossings in the second row are circled in Fig. 3. They arise from $\Delta m = 12$ interactions, and their magnitude can be estimated by comparison with energy spacings at non-avoided crossings in the same K column of Fig. 3.
[c]Avoided crossings in the third and fourth rows arise from $\Delta m = 18$ or 24 interactions and are smaller in magnitude than the avoided crossings in the second row.

value of J observed for that series, and (ii) the effective B values calculated from Eq. [14] for that series must change as smoothly with J as possible in the absence of avoided crossings.

5. DISCUSSION

The main goal of this paper was to study experimentally and theoretically torsion–rotation energy levels above the top of the barrier but below the lowest small-amplitude vibration in acetaldehyde, i.e., the energy levels between V_3 and ν_{10} in Fig. 3. We now have a fairly good understanding of these levels, but some problems remain.

In particular, even though a very large number of trial fits were carried out, with various sets of parameters and various sets of rejected measurements, the magnitude of residuals for microwave transitions involving $v_t = 3$ and 4 was always significantly larger (often exceeding several MHz) than the magnitude of residuals for transitions involving levels with $v_t \leqslant 2$. We thus finally abandoned our original goal of obtaining a fit of the present data set good to experimental error. Since an ''excellent'' fit of levels with $v_t \leqslant 4$ seemed out of reach in the present work, we decided not to invest the large amount of time necessary (i) to arrive at the very best distribution of included versus excluded transitions in the fit, (ii) to reduce the number of adjustable parameters to its absolute minimum, or (iii) to investigate in full detail the possibility of eliminating or floating the two fixed parameters. (We note here in passing that an excellent summary of observed and calculated microwave transition frequencies and intensities of $v_t \leqslant 2$ levels based on the previously achieved fit to experimental error (*5*) has been compiled for radioastronomy purposes (*25*).)

We have come to believe that our $v_t = 3$ and 4 fitting difficulties arise from interactions with the lowest small-amplitude vibrational fundamental ν_{10} at 509 cm^{-1} (584 cm^{-1} in Figs. 1–4 because the torsional zero-point energy must be added). It is still conceivable, however, that inclusion in the data set of additional securely assigned $\Delta K \neq 0$ microwave and infrared transitions involving the $v_t = 3$ and 4 torsional levels (particularly those significantly affected by the various perturbations), together with inclusion in the Hamiltonian of a small number of additional torsion–rotation interaction terms, could lead to a much improved fit.

In any case, further progress in understanding torsion–rotation levels above the barrier in acetaldehyde probably requires (i) new experimental studies aimed at characterizing a number of the mutually interacting $v_t \leqslant 3$ torsion–K-rotation energy level systems predicted by the present molecular constants, and (ii) experimental and theoretical investigation of interactions between the lowest small-amplitude vibrational fundamental and the torsional ''bath-precursor'' states in which it is embedded.

TABLE 12
Two Sets of Interacting $v_t = 3$ Levels ($\Delta K = \pm 1$)[a] and Their Associated B_{eff} Values[b]

v_t	K	JP	Energy	B_{eff}	v_t	K	JP	Energy	B_{eff}	v_t	K	J	Energy	B_{eff}	v_t	K	J	Energy	B_{eff}
3	3	3+	442.403							3	-5	5	491.592						
3	3	4+	445.719	0.414	3	4	4+	443.289		3	-5	6	496.797	0.434	3	-6	6	492.466	
3	3	5+	449.346	0.363	3	4	5+	445.902	0.261	3	-5	7	501.274	0.320	3	-6	7	495.556	0.221
3	3	6+	453.494	0.346	3	4	6+	449.229	0.277	3	-5	8	506.106	0.302	3	-6	8	499.510	0.247
3	3	7+	458.193	0.336	3	4	7+	453.239	0.286	3	-5	9	511.452	0.297	3	-6	9	504.224	0.262
3	3	8+	463.455	0.329	3	4	8+	457.919	0.293	3	-5	10	517.371	0.296	3	-6	10	509.658	0.272
3	3	9+	469.288	0.324	3	4	9+	463.266	0.297	3	-5	11	523.890	0.296	3	-6	11	515.796	0.279
3	3	10+	475.697	0.320	3	4	10+	469.275	0.300	3	-5	12	531.023	0.297	3	-6	12	522.626	0.285

[a]The $v_t = 3$, K = 3 and 4 A+ levels on the left of this table correspond to the minimum of the m = -6 levels in Fig. 3 and to the 3A levels in Fig. 4; the $v_t = 3$, K = -5 and -6 E levels on the right of the table correspond to the minimum of the m = -7 levels in Fig. 3 and to one branch of the 3E levels in Fig. 4.
[b]Given in cm^{-1}, as determined from energy levels in cm^{-1} using Eq. (14). The anomalously large (small) effective B values for the higher-energy (lower-energy) partners on each side of this table suggests a mutual J-dependent repulsion consistent with a $\Delta K = \pm 1$ interaction, but the very large magnitude of the effect near J = K is not yet understood.

ACKNOWLEDGMENTS

The authors are indebted to Drs. R. D. Suenram and F. J. Lovas for making a number of NIST microwave measurements available before publication, and to Drs. A. R. Hight Walker and R. D. Suenram for remeasuring the troublesome ground state $J = 1 \leftarrow 0$ line at 19 265 MHz. The U.S. portion of this work was supported in part by the Division of Chemical Sciences, Office of Basic Energy Sciences, Office of Energy Research, U.S. Department of Energy; the Russian portion was supported in part by the Russian Fund for Fundamental Studies, Grant No. 94-02-05424-a, and the International Science Foundation, Grant R81000; the French portion was supported in part by the G.D.R.P.C.M.G.I. J.-U. G. was supported by a postdoctoral fellowship of the Deutsche Forschungsgemeinshaft. Calculations were carried out at the University of Paris on the IDRIS Computer Center Cray C98 and C94, and at NIST on the Cray YMP.

REFERENCES

1. I. Kleiner, M. Godefroid, M. Herman, and A. R. W. McKellar, *J. Mol. Spectrosc.* **142,** 238–253 (1990).
2. I. Kleiner, J. T. Hougen, R. D. Suenram, F. J. Lovas, and M. Godefroid, *J. Mol. Spectrosc.* **148,** 38–49 (1991).
3. I. Kleiner, J. T. Hougen, R. D. Suenram, F. J. Lovas, and M. Godefroid, *J. Mol. Spectrosc.* **153,** 578–586 (1992).
4. W. L. Barclay, Jr., M. A. Anderson, L. M. Ziurys, I. Kleiner, and J. T. Hougen, *Astrophys. J. Suppl.* **89,** 221–226 (1993).
5. S. P. Belov, M. Yu. Tretyakov, I. Kleiner, and J. T. Hougen, *J. Mol. Spectrosc.* **160,** 61–72 (1993).
6. J. T. Hougen, I. Kleiner, and M. Godefroid, *J. Mol. Spectrosc.* **163,** 559–586 (1994).
7. C. C. Lin and J. D. Swalen, *Rev. Mod. Phys.* **31,** 841–892 (1959).
8. S. P. Belov, V. M. Demkin and M. Yu. Tretyakov, to be submitted for publication.
9. A. F. Krupnov, *Spectrochim. Acta*, in press.
10. A. F. Krupnov, *in* ''Modern Aspects of Microwave Spectroscopy'' (G. W. Chantry, Ed.), pp. 217–256 Academic Press, San Diego, 1979.
11. A. R. Hight Walker and R. D. Suenram, private communication.
12. J. Burie, D. Boucher, J. Demaison, and A. Dubrulle, *J. Phys. (Paris)* **43,** 1319–1325 (1982).
13. A. Bauder and Hs. H. Günthard, *J. Mol. Spectrosc.* **60,** 290–311 (1976).
14. S. P. Belov, M. Yu. Tretyakov, and R. D. Suenram, *Astrophys. J.* **393,** 848–851 (1992).
15. E. Herbst, J. K. Messer, F. C. DeLucia, and P. Helminger, *J. Mol. Spectrosc.* **108,** 42–57 (1984).
16. K. V. L. N. Sastry, E. Herbst, R. A. Booker, and F. C. DeLucia, *J. Mol. Spectrosc.* **116,** 120–135 (1986).
17. K. Nakagawa, S. Tsunekawa, and T. Kojima, *J. Mol. Spectrosc.* **126,** 329–340 (1987).
18. A. G. Ozkabak and L. Goodman, *J. Chem. Phys.* **96,** 5958–5968 (1992).
19. J. Leszczynski and L. Goodman, *J. Chem. Phys.* **99,** 4867–4868 (1993).
20. L. Goodman, J. Leszczynski, and T. Kundu, *J. Chem. Phys.* **100,** 1274–1277 (1994).
21. L. Goodman, T. Kundu, and J. Leszczynski, *J. Am. Chem. Soc.* **117,** 2082–2088 (1995).
22. O. I. Baskakov and M. A. O. Pashaev, *J. Mol. Spectrosc.* **151,** 282–291 (1992).
23. J. Tang and K. Takagi, *J. Mol. Spectrosc.* **161,** 487–498 (1993).
24. J. Ortigoso and J. T. Hougen, *J. Chem. Phys.* **101,** 2710–2719 (1994).
25. I. Kleiner, F. J. Lovas, and M. Godefroid, *J. Phys. Chem. Ref. Data*, in press.